

**Solvent Effect (NMP and DCM) on Morphology and CO₂/CH₄ Separation
Performance of Asymmetric Polysulfone Membranes.**

by

Erry Fareena Ramli

Dissertation submitted in partial fulfilment of

the requirements for the

Bachelor of Engineering (Hons)

(Chemical Engineering)

JULY 2010

Universiti Teknologi PETRONAS

Bandar Seri Iskandar

31750 Tronoh

Perak Darul Ridzuan

CERTIFICATION OF ORIGINALITY

This is to certify that I am responsible for the work submitted in this project, that the original work is my own except as specified in the references and acknowledgements, and that the original work contained herein have not been undertaken or done by unspecified sources or persons.



Erry Fareena Ramli

CERTIFICATION OF APPROVAL


**Solvent Effect (NMP and DCM) on Morphology and CO₂/CH₄ Separation Performance of
Asymmetric Polysulfone Membranes.**

by

Erry Fareena Ramli

**A Project Dissertation Submitted to the
Chemical Engineering Programme
Universiti Teknologi Petronas
A Partial Fulfilment of the Requirements for the
Bachelor of Engineering (Hons)
(Chemical Engineering)**

Approved by;



Assoc. Prof. Dr. Zakaria Man
Chemical Engineering Department
Universiti Teknologi PETRONAS
Dr. Zakaria Man

**UNIVERSITI TEKNOLOGI PETRONAS,
TRONOH, PERAK.**

JULY 2010

ABSTRACT

Performance of a membrane is strongly influenced by the morphology of the membrane itself. The choice of the solvent used is very critical process. The objectives of this project is to study the effect of solvents which are DCM (dichloromethane) and NMP (N-methyl pyrrolidone) in membrane preparation on the morphologies of membrane and its relation to carbon dioxide and methane separation characteristic.

Membrane will be fabricated using wet phase inversion technique. The polymer used is polysulfone (PSF) while the non-solvents are ethanol and water and were chosen on the basis of the solubility parameter map. The membranes will be characterized in term of the cross-sectional morphology as well as the gas permeability. Characterization will be conducted by using SEM to analyse the morphology, FTIR to measure molecular interactions and UTM to measure the mechanical properties. Gas permeation unit will be used to evaluate the performance of membrane by applying different feed pressure. The performance of membranes will be evaluated by measuring CO₂ and CH₄ permeances as well as CO₂/CH₄ ideal selectivity.

Therefore, the understanding of mechanism of membrane formation is very crucial in order to produce desirable morphology that leads to enhancement of the membrane performance in pure gas separation process.

ACKNOWLEDGEMENTS

First and foremost, I would like to give my sincere thanks to ALLAH SWT, the almighty God, the source of my life and hope for giving me the strength and wisdom to complete the research.

I am most grateful to my supervisors Dr Farooq Ahmad and Dr. Zakaria Man for their patience and constant encouragement until this project is successfully completed. I would like to thank the coordinators of Final Year Project I and II, Dr. Suriati Sufian and Dr. Khalik Mohamad Sabil for their suggestions, criticisms and helps.

I also would like to express my gratitude to all technologists from UTP, Mr. Jailani, Mr. Irwan, Ms Norhazneyza, Mr. Paris, Mr. Firdaus and Mr. Shaharuddin for their effort in helping and providing me with the all chemicals and other experimental tools that I need for this research. Special thanks also to my undergraduate friends for their encouragement and friendship.

At last and most importantly, I would like to thank my family for their open-mindedness and endless support. They are always close to my heart.

TABLE OF CONTENTS

CERTIFICATION OF ORIGINALITY.....	i
CERTIFICATION OF APPROVAL	ii
ABSTRACT	iii
ACKNOWLEDGEMENTS	iv
TABLE OF CONTENTS	v
LIST OF FIGURES.....	viii
LIST OF TABLES.....	ix
ABBREVIATIONS.....	x
NOMENCLATURES	xi
CHAPTER 1.....	1
INTRODUCTION	1
<i>1.1 Carbon Dioxide in Natural Gas Processing</i>	<i>1</i>
<i>1.2 Recent Technologies in Carbon Dioxide Removal from Natural Gas</i>	<i>2</i>
1.2.1 Absorption	2
1.2.2 Adsorption	2
1.2.3 Membrane Technology.....	3
1.3 Problem Statement.....	4
1.4 Objective of Research	6
1.5 Scope of Study.....	7
1.5.1 Fabrication of Asymmetric Polycarbonate Membrane	7
1.5.2 Characterization of Asymmetric PC Membrane	7
1.5.3 Evaluation of Asymmetric PC Membrane Performance	7
1.6 Organization of This Thesis	8
CHAPTER 2.....	9
LITERATURE REVIEW	9
2.1 Membrane Definition and Classification.....	9
2.1.1 Types of Membrane.....	10
2.1.2 Membrane Fabrication	12
2.2. Effect of Solvent on Membrane Morphologies and Transport Properties	13
2.3 Membrane Characterization.....	14
2.3.1 Characterization of Cross-section of Membrane Structures	14

2.3.2 Porosity Determination	14
2.4 Membrane Materials for CO ₂ /CH ₄ Separation.....	16
2.4.1 In-organic Membrane for CO ₂ /CH ₄ Separation.....	16
2.4.2 Polymeric Material for CO ₂ /CH ₄ Separation	16
2.4.3 Solvents used	19
CHAPTER 3.....	21
THEORY	21
3.1 Formation of Phase Inversion-Based Asymmetric Membrane.....	21
3.2 Ternary Phase Diagram	23
3.3 Prediction of Solubility Parameter	25
CHAPTER 4.....	28
METHODOLOGY	28
4.1 Coagulation Value Determination	28
4.2 Membrane Fabrication	29
4.2.1 Experimental.....	29
4.3 Membrane Characterization.....	31
4.3.1 Scanning Electron Microscopy (SEM)	31
4.3.2 Porosity Calculation	31
4.3.3 Gas Permeation Studies.....	32
4.3.4 Molecular Interactions.....	33
4.3.5 Mechanical Properties	34
4.4 Tools and Equipment	35
4.4.1 Lab tools and equipments for membrane fabrication;.....	35
4.4.2 Equipments for characterization;	35
4.5 Key Milestones.....	36
4.6 Gantt Chart.....	37
CHAPTER 5.....	38
RESULT AND DISCUSSION	38
5.1 Formation and Morphologies of Asymmetric PSF Membrane	38
5.1.1 Effect of Solvents	38
5.2 CO ₂ /CH ₄ Separation Characteristic.....	45
5.2.1 Effect of Solvents	45
5.3 Molecular Interactions.....	48
5.4 Mechanical Strength.....	50

CHAPTER 6.....	53
CONCLUSION AND RECOMMENDATION	53
APPENDICES.....	xii
<i>APPENDIX A: Raw Material Properties</i>	<i>xii</i>
A.1 Polymer.....	xii
A.2 Chemicals.....	xii
<i>APPENDIX B: Solubility Parameter</i>	<i>xiii</i>
B.1 Solubility Parameter of Pure Components	xiii
B.2 Solubility Parameter of Mixtures.....	xiii
B.3 Solubility Parameter Difference Calculation ($\Delta\delta$)	xv
<i>APPENDIX C: Porosity Calculation</i>	<i>xvii</i>
C.1 Thickness of Membrane	xvii
C.2 Membrane Overall Porosity Calculation.....	xvii
<i>APPENDIX D: Coagulation Value</i>	<i>xix</i>
D.1. Coagulation Value at Various Solvent – Non-solvent Pair	xix
<i>APPENDIX E: Gas Permeation.....</i>	<i>xx</i>
E.1 Gas Permeance and CO ₂ /CH ₄ Ideal Calculations.....	xx
E.2 Data of Permeation Results	xxii
<i>APPENDIX F: Mechanical Strength –UTM Results.....</i>	<i>xxvi</i>
<i>APPENDIX G: FTIR Results</i>	<i>xxix</i>
REFERENCES	xxxiii

LIST OF FIGURES

Figure 2.1: Schematic Diagrams of the Principal Types of Membranes	10
Figure 3.1 Schematic Phase Diagram	24
Figure 4.1 Gantt Chart	37
Figure 5.1 SEM images	38-39
Figure 5.2 Solubility parameter difference between solvent to coagulant and solvent to polysulfone	41
Figure 5.3 Coagulation value and solubility parameter difference of solvent mixtures and coagulant	43
Figure 5.4 CO ₂ permeance of membranes prepared from different solvent mixtures at various feed pressures.	45
Figure 5.5 CH ₄ permeance of membranes prepared from different solvent mixtures at various feed pressure	46
Figure 5.6 CO ₂ /CH ₄ ideal selectivity of membranes prepared from different solvent mixtures at various feed pressures.	47
Figure 5.7 FTiR Result	48-49
Figure 5.8 Strength at Break (N/m)	50
Figure 5.9 Strength at Yield (N/m)	51
Figure 5.10 Elastic Modulus (N/m)	51
Figure F.1 Tensile Test	xxvi-xxvii
Figure G.1 FTiR Results	xxix-xxxii

LIST OF TABLES

Table 4.1: Sample Compositions of Polymer Solutions	28
Table 4.2 Membrane Fabrication Calculation	39
Table 4.3 Key Milestones	36
Table 5.1 Membranes porosity prepared using different solvent mixture.	40
Table 5.2 Solubility parameter of PSf, solvents and coagulant mixtures	41
Table 5.3 Strength of Material of Membranes	50
Table A.1 Properties of Polymer	xii
Table A.2 List of properties of pure components	xii
Table B.1 Solubility parameter of pure components (Hansen, 2000)	xiii
Table B.2 Data tabulation for the total volume, V , and volume fraction, ϕ , of solvent mixtures.	xiv
Table C.1 Thickness of membrane measured using SEM	xvii
Table D.1 Coagulation value of different solvent mixtures	xix
Table E.1. Gas permeation results for NMP 100 w% membrane	xxii
Table E.2. Gas permeation results for NMP 75 w% / DCM 25w% membrane	xxiii
Table E.3. Gas permeation results for NMP 50w% / DCM 50w% membrane	xxiv
Table E.4. Gas permeation results for DCM 100 w% membrane	xxv
Table F.1 UTM Testing Data Extraction	xxviii

ABBREVIATIONS

FTIR	Fourier Transform Infrared Spectroscopy
IUPAC	International Union of Pure and Applied Chemistry
SEM	Scanning Electron Microscope
SG	Specific Gravity
UTM	Universal Testing Machine

Chemical Name

CH ₄	Methane
CO ₂	Carbon Dioxide
CMS	Carbon Molecular Sieve
DCM	Dichloromethane
EtOH	Ethanol
H ₂ O	Water
H ₂ S	Sulfuric Acid
N ₂	Nitrogen
NMP	N-Methylpyrrolidone
O ₂	Oxygen
PES	Polyethersulfone
PSF	Polysulfone
SO ₂	Sulfur Dioxide

NOMENCLATURES

A	Membrane area	(cm^2)
$\alpha_{i/j}$	Ideal selectivity of component i over component j	$(-)$
δ	Overall solubility parameter	$(\text{J}^{1/2}/\text{cm}^{3/2})$
δ_{mix}	Overall solubility parameter of solvent mixtures	$(\text{J}^{1/2}/\text{cm}^{3/2})$
δ_d	Solubility parameter for dispersive component	$(\text{J}^{1/2}/\text{cm}^{3/2})$
δ_p	Solubility parameter for polar component	$(\text{J}^{1/2}/\text{cm}^{3/2})$
δ_h	Solubility parameter for hydrogen bonding component	$(\text{J}^{1/2}/\text{cm}^{3/2})$
$\Delta\delta$	Solubility parameter difference	$(\text{J}^{1/2}/\text{cm}^{3/2})$
ε	Porosity	$(\%)$
l	Membrane thickness	(cm)
p	Pressure	(bar)
P	Permeability	$(\text{cm}^3(\text{STP}).\text{cm}/\text{cm}^2.\text{s}.\text{cmHg})$
P/l	Permeance	$(\text{cm}^3(\text{STP})/\text{cm}^2.\text{s}.\text{cmHg})$
ρ	Density	(g/cm^3)
Q	Volumetric flow rate	(cm^3/s)
Q_{stp}	Volumetric flow rate at standard temperature and pressure	$(\text{cm}^3(\text{STP})/\text{s})$
t	Time	(s)
T	Temperature	(K)
T_g	Glass transition temperature	(K)
V	Molar volume	(cm^3/mol)
ϕ	Volume fraction	$(-)$

CHAPTER 1

INTRODUCTION

1.1 CARBON DIOXIDE IN NATURAL GAS PROCESSING

Natural gas is the cleanest, safest, and most useful of all energy sources. It is used as a feedstock for petrochemical plant or as fuel in power generation plant and vehicles. The various uses of natural gas have increased the consumption of natural gas. Consequently, natural gas production must be increased in order to meet the increasing demand of natural gas.

Natural gas composition may vary from one source to another. Basically, methane is the major component in natural gas, comprising typically 75-90% of the total component (Baker, 2004). Natural gas also contains significant amount of ethane, propane, butane and other higher hydrocarbons. In addition, natural gas may also contain undesirable impurities such as carbon dioxide and hydrogen sulfide (Baker, 2004). All of these impurities need to be separated from natural gas in order to meet the pipeline specification for natural gas delivery.

One of the impurities that need to be separated from natural gas is carbon dioxide. It is well known that carbon dioxide in the presence of water is highly corrosive that can rapidly destroy the pipeline and equipment system. Specifically for LNG plant, the natural gas is cooled down to very low temperature that can make CO₂ become solid. However for pipeline transportation, the solidification of CO₂ must be prevented as it may block the pipeline system and cause transportation problem. The presence of CO₂ will also reduce the heating value content of natural gas and eventually the selling price of natural will be lowered. Therefore, CO₂ removal from natural gas is necessary in order to improve the quality of natural gas produced.

1.2 RECENT TECHNOLOGIES IN CARBON DIOXIDE REMOVAL FROM NATURAL GAS

Currently, the available technologies for natural gas processing are amine-based or hot potassium carbonate-based absorption process, adsorption technology, and membrane technology. However, each of these technologies has some limitation for removing CO₂ from natural gas. Most commercial processes to remove acid gas in bulk quantity involve the use of amine, usually alkanolamines, as chemical solvent in absorption technology due to its outstanding performance (Kohl and Reisenfeld, 1979).

1.2.1 Absorption

Generally absorption could cause pollution by corrosive amine disposal which is used as the absorbent (Bord, *et al.*, 2004). Consequently, anti corrosion agent must be frequently injected in order to avoid corrosion. Although it can be recycled, there is still small amount that need to be treated and disposed properly to save the environment.

1.2.2 Adsorption

There are two types of adsorption which are Thermal Swing Adsorption (TSA) and Pressure Swing Adsorption (PSA). In TSA process, desorption takes place at temperatures much higher than adsorption. Increasing temperature is required to shift the adsorption equilibrium and cause the regeneration of the adsorbent. TSA needs long cycle time as time required to heat, desorb, and cool a bed is usually in the range of a few hours to over a day. Therefore, TSA is exclusively used to remove small concentrations of impurities from feeds due to this cycle time limitation (Keller, 1987). Besides long cycle time, TSA also requires high energy supply and suffer from large heat loss. PSA process is quite similar to TSA except the regeneration of adsorbent is done by applying reduced pressure of system. On the contrary, PSA has short cycle time as time required to load, depressurize, regenerate, and repressurize a bed but it needs high pressure and vacuum pressure which contribute to the high operating cost.

1.2.3 Membrane Technology

Existing CO₂ removal technologies such as amine stripping, PSA and TSA are still suffering from several shortcomings. Those technologies consume large space, high capital and operating cost. Since the last two decades, membrane technology has been developed to face these challenges. This technology is based on the ability of CO₂ and other components of natural gas in passing through a thin membrane barrier. The mixture of gases will be separated into permeate and retentate stream. The highly permeating component will diffuse through the membrane and separated from the non-permeable component.

Membrane technology offers some advantages over other conventional CO₂ removal technologies which are environmental friendly, lower capital cost, low energy consumption, space efficiency and also suitable for remote location application. However, the application of membrane for gas separation, particularly for CO₂ removal, is relatively new as compared to other existing technologies. Unlike other gas separation using membrane technology such as hydrogen separation from methane and nitrogen or nitrogen enrichment from air, CO₂ removal using membrane technology still requires much improvement in term of stability and separation performance in order to be able to compete with current CO₂ removal technologies.

Even though some membrane units have been used commercially, membrane technology is still a minor player in CO₂ removal from natural gas. Low stability for long-term usage and highly sensitive to the presence of impurities other than CO₂ and/or H₂S in natural gas become major problems when membrane is used for this application. In addition, single stage of membrane unit is not economically applicable to be applied for large flow rate of feed gas (greater than 30 MMscfd) as high loss of desired product such as methane may be taken place (Baker, 2004). Two stage or even three-stage of membranes unit are commonly required to reduce loss of methane. However, it will add more complexity of membrane plant and increase the operating cost as recompression cost must be considered. Generally, current membrane technology to remove high concentration of CO₂ (more than 10%) from natural gas to meet the pipeline specification (CO₂ content lower than 2%) is still too expensive to compete head-to-head with amine plants (Baker, 2004). Therefore, further improvement is required to enhance the performance of gas separation using membrane so that membrane becomes a viable technology in future.

1.3 PROBLEM STATEMENT

Polymeric membrane is not fully commercialized in natural gas separation industries as it is highly sensitive to impurities other than CO₂ and H₂S and low stability for long term usage and non-economical to be applied for large flow rate of feed gas (Baker, 1994).

Basically, the performance of a membrane is assessed according to permeability and selectivity. High permeability leads to higher productivity and lower cost while high selectivity contributes to more efficient separation and higher recovery. One of the limitation in gas separation membrane technology is that the difficulty to achieve both high permeability and selectivity at the same time. High permeability is usually followed by low selectivity and vice versa.

Asymmetric membrane has been extensively studied for gas separation process. It consists of a thin-skin layer supported by porous sub-layer in which both layers are composed of the same material. This type of membrane is developed usually to increase flux or permeability of gas and to obtain high selectivity at the same time. The thin-skin layer of the asymmetric membrane functions as a selective barrier while the porous sub-layer serves only for mechanical strength with negligible effects on separation.

The asymmetric membrane morphologies and properties are influenced by the process condition applied upon fabrication stage. There are some parameters involved in controlling the membrane morphology during fabrication stage such as polymer concentration, non-solvent concentration, solvent/non-solvent pair, humidity, evaporation time, etc (Mulder, 1996). As the morphology of membrane formed could vary greatly due to different condition of the fabrication process, it is crucial to understand the effect of these preparation parameters on the mechanism of asymmetric membrane formation in order to produce desired morphologies and its relation to the performance in removing CO₂. Hence, a comprehensive study of fabrication process is necessary in order to produce asymmetric membrane suitable for gas separation.

It is known that the mutual affinity between solvent-coagulant and solvent-polymer are the key points to obtain the desired structures in the membrane (Mulder, 1997). The difference between the solubility parameter is related with the mutual affinity of both compounds. The

increase of solubility parameter difference means the decrease of the mutual affinity (Matsuyama, *et al.*, 2001) When the mutual affinity of solvent-coagulant is low, the outflow of solvent into coagulant decreases, produces less porous membrane structure. Meanwhile, high mutual affinity of solvent-polymer, produces less porous membrane structure. Matsuyama, *et al.* (2002) studied the preparation of porous cellulose acetate membranes using four organic solvents in the preparation of the casting solution and noted that as the mutual affinity between the solvent and coagulant decreased, the membrane porosity and the average pore size increased. More recently, Temtem, *et al.* (2006) produced PSF membranes from six different solvents showed that the high mutual affinity between solvent and polymer produced the less pore size. Reverchon, *et al.* (2006) studied the production of poly(methyl methacrylate) membranes and evidenced similar results.

The experimental results of many system show that systems those exhibiting instantaneous demixing often form more pores and macrovoids, while delayed onset demixing process form less pores and macrovoids. This means that the parameters that favour the formation of porous membranes may also favour the formation of macrovoids (Mulder, 1996). The presence of macrovoid is not generally favourable, because they may lead to a weak spot in the membrane especially when high pressures are applied in gas separation.

In this study, polysulfone was selected as membrane forming material. This is because certain properties of polysulfone are found suitable for the application of CO₂ removal from natural gas such as high glass transition temperature (T_g), (185 °C) which makes it high thermal resistance material, and low rigidity but with free space available due to the presence of aromatic ring, good control or pore size and pore size distribution, high membrane strength and good film-forming properties. In addition, polysulfone is relatively cheap compared to polyimide.

Some works have been carried out in the past to study polysulfone-based membrane for gas separation. It focused on sorption and transport properties of dense polycarbonates membrane (Koros, *et al.*, 1977; Wonders, 1979; Jordan and Koros; 1990; Chen *et al.*, 2000) and gas permeation properties of asymmetric polycarbonate (Pinnau, 1992). However, no works have been reported on the effect of solvent which are NMP and DCM on the morphology and CO₂ separation performance of asymmetric polysulfone membrane. Therefore, study on the effect of solvent to produce desired morphologies of asymmetric

membrane using alternative material such as polysulfone (PSf) for the application of CO₂ removal from CH₄ is important.

1.4 OBJECTIVE OF RESEARCH

The main objectives of this research are:

1. To synthesis PSF membrane by two different solvents which are NMP and DCM at different concentration.
2. To investigate the effect of solvent on the morphologies of asymmetric PSf membrane.
3. To evaluate the performance of asymmetric PSf membrane in term of CO₂ and CH₄ permeance as well as CO₂/CH₄ ideal selectivity.

1.5 SCOPE OF STUDY

The scope of this research is divided into the following section:

1.5.1 Fabrication of Asymmetric Polycarbonate Membrane

Polysulfone (PSf) would be used as membrane forming material during asymmetric membrane fabrication. N-Methyl Pyrrolidone (NMP) and Dichloromethane (DCM) were selected as solvents meanwhile water and ethanol were used as coagulants. Fabrication of asymmetric PSf membrane would be carried out via wet phase inversion process by varying-solvent concentration. In addition, solubility parameter and coagulation value of phase separation process were also determined in order to understand the mechanism of membrane formation.

1.5.2 Characterization of Asymmetric PC Membrane

Characterizations of asymmetric PSf membranes were carried out by using some characterization tools such as SEM, FTiR and UTM. SEM was used to study the sub-structure beneath of all asymmetric PC membranes prepared from different solvent mixture while the mechanical properties is measured using UTM and molecular interaction is measured using FTiR.

1.5.3 Evaluation of Asymmetric PC Membrane Performance

The performance of asymmetric PSf membrane would be evaluated by determining the CO₂ and CH₄ permeance as well as CO₂/CH₄ ideal selectivity at various feed pressure ranging from 1 to 5 bar. Downstream pressure and operating temperature were assumed constant at 1 bar and room temperature, 25°C, respectively. The volume of permeate collected would be used to determine the gas permeance and CO₂/CH₄ ideal selectivity.

1.6 ORGANIZATION OF THIS THESIS

This thesis is divided into following chapters. Chapter 1 describes the research background related to common problems in natural gas treating process with regard to the presence of acid gases particularly for CO₂. The advantages and disadvantages of existing CO₂ separation technology such amine-based absorption, adsorption and membrane technology were also presented in this chapter. This chapter also presents problem statement, objectives of research and scope of study of this work.

Chapter 2 reviews the past and current research work pertaining to membrane development. It covers information on membrane definition and classification, development of asymmetric membranes, membrane characterization technique and various membrane materials for CO₂/CH₄ separation.

Chapter 3 describes in detail on the phase inversion method for making asymmetric membranes. This chapter also presents some factors affecting membrane morphologies, solubility parameter, polymer properties and transport phenomena on asymmetric membrane.

Chapter 4 discusses the material, preparation and fabrication technique applied in this study in order to produce asymmetric polycarbonate membrane. It also describes in detail on procedure to determine coagulation value and in setting up some analytical tools such as SEM, FTiR and UTM. This chapter covers the testing procedure to study gas separation performance in terms of CO₂/CH₄ permeance and CO₂/CH₄ ideal selectivity at various feed pressures.

Chapter 5 discusses all the experimental results obtained in this work. It includes the relationship between solubility parameter of casting solution and coagulation value on the SEM images of membrane produced. The different morphologies of asymmetric PC membranes formed were correlated with the membrane performance in term of CO₂, CH₄ permeance and ideal selectivity of CO₂/CH₄ at various feed pressure. Finally, FTiR and UTM results of membranes are also discussed in this chapter.

Chapter 6 contains concluding remarks along with the recommendations for future work.

CHAPTER 2

LITERATURE REVIEW

2.1 MEMBRANE DEFINITION AND CLASSIFICATION

The primary role of a membrane is to act as a physical permselective barrier. Excluding the biological aspect, a membrane is a layer of material which serves as a selective barrier between two phases and remains impermeable to specific particles, molecules, or substances when exposed to the action of a driving force. The thin film in either solid or liquid state act as a permselective barrier for gaseous, liquid, or solid permeant.

Definitions;

1) *Membrane is an interphase which restricts the transport of matter and/or energy between two adjacent outer phases in a very specific way (Strathmann, et al, 1989).*

2) *Membrane is a phase that acts as a barrier to prevent mass movement but allows restricted and/or regulated passage of one or more species through it. (Lakshminarayanaiah, 1984).*

Some components are allowed passage by the membrane into a permeate stream, whereas others are retained by it and accumulate in the retentate (Zydney and Zeman, 1996). Separation of a mixture is achieved when some components permeate the membrane more freely than others due to the permeability difference.

Membranes can be of various thickness, either molecularly homogenous, i.e., completely uniform in concentration and structure; or the interface may be chemically or physically heterogeneous, e.g., containing holes or pores of finite dimensions or consisting of some form of layered structure (Baker, 1994).

A normal filter meets this definition of a membrane but by convention the term filter is usually limited to structures that separate particulate suspensions larger than 1 to 10 μ m. According to IUPAC, there are three different types of pore size classifications: microporous ($d_p < 2\text{nm}$), mesoporous ($2\text{nm} < d_p < 50\text{nm}$) and macroporous ($d_p > 50\text{nm}$) (Younan, et al., 2003).

Membranes can be neutral or charged, and particles transport can be active or passive. The latter can be facilitated by pressure, concentration, chemical or electrical gradients of the membrane process. Membranes can be generally classified into three groups: inorganic, polymeric or biological membranes. They differ significantly in their structure and functionality (Mulder, 1996).

2.1.1 Types of Membrane

Generally, there are two types of membranes which are symmetric and asymmetric membranes (Mulder, 1996). Symmetric membranes have essentially same structure and transport properties throughout its thickness while asymmetric membrane constituted two or more structural planes of non-identical morphologies (Koros, *et al.*, 1996). The dense and thin skin layer is for the separation of a mixture while the porous sub-layers is to provide mechanical strength to the membrane (Ismail, *et al.*, 2004).

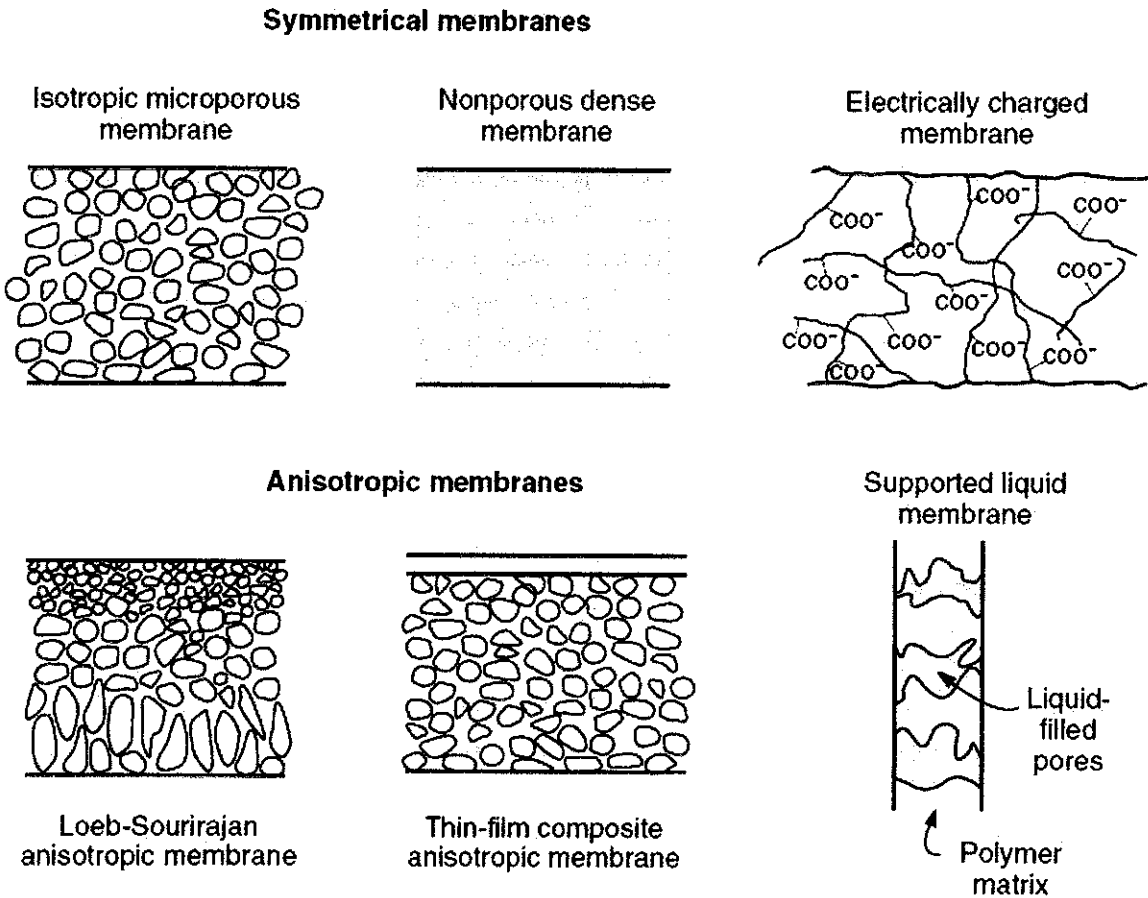


Figure 2.1 Schematic Diagrams of the Principal Types of Membranes

The porosity of the sublayer increases across the membrane from top to bottom. The separation characteristic are governed by the nature of the skin polymer or pore size and the mass transport rate mainly by the thickness. In general, the mass transport rate is inversely proportional to the thickness of the actual skin layer. The porous sublayer serves only as a support for the skin layer and has very little effect on the separation characteristics and mass transport rate of membrane.

2.1.2 Membrane Fabrication

It is very crucial to enhance the membrane performance to make membrane becomes an effective technology in future. Membrane characterization has to be done to study the mechanism of membrane formation and to relate their morphologies and properties to the membrane separation properties.

In preparing the synthetic membrane, a number of different techniques are available such as stretching, sintering, track etching, phase inversion, template leaching, and solution coating.

-Sintering

It involves compressing a powder consisting of particles of a given size and sintering at elevated temperature to obtain porous membranes from organic or inorganic materials.

-Stretching

An extruded film or foil made from a partially crystalline polymeric material is stretched perpendicular to the direction of the extrusion, so that the crystalline regions are located parallel to the extrusion direction.

-Track Etching

A way to obtain an assembly of parallel cylindrically shaped pores of uniform dimension.

-Template Etching

It is done by leaching out one of the components from a film to prepare porous membranes.

-Phase Inversion

It is a process whereby a polymer is transformed in a controlled manner from a liquid to a solid state.

-Coating

Dense polymeric membranes in which transport takes place by diffusion generally show low fluxes.

Only through the use of phase inversion process, it is possible to produce either open or dense structures while others can only produce either open or dense structures. Phase inversion concept covers various ranges of techniques and one of the most common techniques is immersion precipitation (Mulder, 1996).

2.2. EFFECT OF SOLVENT ON MEMBRANE MORPHOLOGIES AND TRANSPORT PROPERTIES

Selection of the solvent plays a vital role in controlling the membrane morphologies and properties. Iqbal, *et al.* (2008) found that DCM-based polycarbonate membranes have more porous substructure than that of chloroform-based membrane for any non solvents used. This is due to the fact that DCM has smaller solubility parameter difference with coagulant as compared to chloroform.

Different morphologies of asymmetric membranes develop because of varying rates of demixing of the casting solution. Fast demixing of the casting solution produces a highly porous membrane with the present of the macrovoids while delayed demixing of casting solution leads to less porous and macrovoid free substructure of a membrane. In order to understand the fast and delayed demixing mechanism of casting solution in preparing membranes using wet phase inversion method, the effects of immersion precipitation step on the change of membrane structure must be considered.

Hwang, *et al.* (1996) has studied about the combination of cosolvent in Polyethersulfone (PES) membrane development. Since DCM is a weak solvent to PES, the thermodynamic quality of the PES-DCM membrane is low. PES membranes was, however, more likely dependent upon the solvent evaporation from the casting solution/air interface rather than the change of thermodynamic quality of the casting solution. Structure of PES membrane prepared with pure NMP solution has high thermodynamic quality. Finger-like macrovoids were well developed, which is the typical structure of micro/ultrafiltration membranes of high permeability while it is vice versa for membrane prepared from DCM solvent.

2.3 MEMBRANE CHARACTERIZATION

Membrane may differ significantly in their morphologies and properties and consequently in their application (Mulder, 1996). Therefore, membrane needs to be characterized in order to study the mechanism of membrane formation and to relate their morphologies and properties to the membrane separation properties. There are variety of techniques that can be utilized to characterize the morphologies and properties of membrane. Several techniques on the membrane characterization such as cross-sectional images of membrane and porosity determination will be discussed briefly on the following section.

2.3.1 Characterization of Cross-section of Membrane Structures

Scanning Electron Microscopy (SEM) has been used extensively by many researchers to obtain a sophisticated image of membrane structures (Kesting, 1990; Shieh *et al.*, 1998; Niwa *et al.*, 2000; Wang *et al.*, 2006). Characterizing non-conductive membrane using SEM requires coating treatment in order to make sample become highly conductive. The coated membrane samples are observed by varying the magnification of images. The SEM technique can be used to obtain cross-sectional images of membrane structure.

2.3.2 Porosity Determination

Porosity determination of gas separation membrane can be carried out using overall porosity formula as reported by other researchers (Chun *et al.*, 2000; Jansen *et al.*, 2005a; Jansen *et al.*, 2005b; Macchione *et al.*, 2006). Porosity of membrane is estimated by measuring the thickness (l) and area (A) of membrane, mass (m) of sample and density (ρ) of the respective polymer. The overall porosity formula is described as follows:

$$\varepsilon = \frac{V_{void}}{V_{tot}} = \frac{IA - (m / \rho)_{pol}}{IA} \quad (2.1)$$

Calculating the porosity of membrane using this formula require accurate reading of membrane thickness. Measurement of membrane thickness can be determined using SEM or micrometer gauge (Jansen *et al.*, 2005a; Macchione *et al.*, 2006). Careful treatment must be taken into account as thickness of membrane could be reduced due to too much force while preparing sample for SEM and micrometer measurement.

2.4 MEMBRANE MATERIALS FOR CO₂/CH₄ SEPARATION

There are two type of materials that can be used for gas separation i.e., polymeric and inorganic material. Each type of material has its own characteristics and advantages for gas separation application. A brief discussion of inorganic and polymeric membrane will be given in Sections 0 and 0.

2.4.1 Inorganic Membrane for CO₂/CH₄ Separation

Inorganic membranes offer good performance in high thermal resistance, high stability, permeability as well as selectivity. Like organic membranes, inorganic membranes are also categorized as dense membrane and porous membranes. Porous inorganic membranes consist of symmetric and asymmetric. Since low flux or permeability resulted from dense membrane, therefore most of the research works were conducted on porous inorganic membranes such as carbon and zeolite membrane.

2.4.2 Polymeric Material for CO₂/CH₄ Separation

Even though inorganic membranes show some promises separation for CO₂ separation from natural gas but low reproducibility for large scale production and high cost of fabrication are two problems encountered when using this material. Thus, most commercial and research works on gas separation membranes are reported to be concentrated on polymeric material (Nunes and Peinemann,2001). Some polymers that have been widely studied as polymeric material for gas separation membrane will be discussed further in the following section.

2.4.2.1 Cellulose Acetate Membrane

Cellulose acetate is one of the membrane materials that has been used in industry for the separation of CO₂ from natural gas (Dortmundt, *et al.*, 1999). Cellulose acetate is used because it is inexpensive and has the properties suitable for CO₂ separation (Li, *et al.*, 1998).

Although the cellulose acetate has been used commercially for CO₂/CH₄ separation, their use for gas separation is characterized by the following drawbacks (Peinemann, *et al.*, 1988):

- a) sensitivity to condensed water
- b) sensitivity to microbiological attack
- c) highly plasticized particularly during CO₂ separation
- d) low heat resistance (up to 70°C)
- e) relatively high manufacturing cost, because cellulose acetate cannot be directly air-dried (if direct air drying is employed, the porous base layer will collapse)

2.4.2.2 Polycarbonate

Polycarbonate-based membranes have been studied for many applications of gas separation. Some studies have also been carried out to investigate the application of polycarbonate membrane for CO₂/CH₄ separation (Koros *et al.*, 1977; Jordan *et al.*, 1990). Introducing other material such as polypyrrole to form mixed matrix membrane or applying post-treatment method such as annealing after membrane fabrication do not give any significant impact in order to enhance the performance of membrane.

2.4.2.3 Polyimide Membrane

Rigid glassy polymers, availability of bulky groups and high glass transition temperature (T_g), chemical resistance and mechanical strength are some typical properties of this material.

Dianhydride (Ar) and diamine (R) portion play important role in enhancing the performance of polyimide-based membrane. Several generalities can be taken to describe the diamine portion in polyimide-based membrane (Gosh and Mital, 1996).

- a) Increasing the monomer rigidity decreases permeability but increase the selectivity.
- b) The presence of CF_3 group in monomer increases the permeability
- c) The presence of a dimethylsiloxyl component in polyimide increases permeability but decreases selectivity.

However, polyimide is very susceptible to plasticization when CO_2 is present in the feed (Shekhawat, 2003). In addition, polyimide material is expensive as compared to other polymeric materials. Therefore, the application of CO_2 removal using polyimide-based membrane is still limited.

2.4.2.4 Polysulfone

PSF is a standard membrane material and used widely in industry since it has satisfactory gas permeabilities, low cost, acceptable permselectives and resist to highly sorbing, plasticizing gases. It contains the subunit aryl- SO_2 -aryl, the defining feature of which is the sulfone group. These polymers are rigid, high-strength, and transparent, retaining its properties between $-100^\circ C$ and $150^\circ C$. Polysulfone allows easy manufacturing of membranes, with reproducible properties and controllable size of pores down to 0.04 microns. Such membranes can be used in applications like hemodialysis, waste water recovery, food and beverage processing, and gas separation.

Generally, it is noticeable that the performance of PSf membranes as reported by other researchers is still inferior as compared to other membrane material such as polyimide.

Therefore, study on solvent effect to improve the performance of PSf membrane in separating CO₂ from CH₄ is still highly necessary.

2.4.3 Solvents used

The solvent exchange process and its kinetic between the membrane and the quench bath have a great influence on the formation of undesired macrovoids and uncontrolled skin thickness. It is not easy, however, to evaporate those solvents from the casting solution/air interface owing to their poor volatilities. DCM is a volatile and weak solvent while NMP is nonvolatile solvent. PSF dissolved differently in these two solvents, therefore PSF solubility in solvent system is controlled by changing the ratio between this DCM and NMP.

N-Methyl-2-pyrrolidone (NMP) is a chemical compound with 5-membered lactam structure. It is a clear to slightly yellow liquid miscible with water and solvents like ethyl acetate, chloroform, benzene and lower alcohols or ketones. It also belongs to the class of dipolar aprotic solvents which includes also dimethylformamide, dimethylacetamide and dimethyl sulfoxide. Other names for this compound are: 1-methyl-2-pyrrolidone, N-methyl-2-pyrrolidinone, and m-pyrrole, and pharماسolve.

N-Methylpyrrolidone is used to recover pure hydrocarbons while processing petrochemicals (such as the recovery of 1,3-butadiene using NMP as an extractive distillation solvent) and in the desulfurization of gases. Due to its good solvency properties N-methyl-2-pyrrolidone is used to dissolve a wide range of chemicals, especially in the polymers field. It also used as a solvent for surface treatment of textiles, resins and metal coated plastics or as a paint stripper.

World production capacity for NMP was 226 million lb in 2006. NMP has desirable properties such as low volatility, low flammability, and relatively low toxicity. However, it has been identified as a reproductive toxicant, first by California in 2001 and then by the European Commission in 2003.

Dichloromethane (DCM or methylene chloride) is the organic compound with the formula CH₂Cl₂. This colorless, volatile liquid with a moderately sweet aroma is widely used as a

solvent. More than 500,000 tons were produced in 1991. Although it is not miscible with water, it is miscible with many organic solvents (Rossberg, *et al.*). It was first prepared in 1840 by the French chemist Henri Victor Regnault, who isolated it from a mixture of chloromethane and chlorine that had been exposed to sunlight.

Dichloromethane's volatility and ability to dissolve a wide range of organic compounds makes it a useful solvent for many chemical processes. It is widely used as a paint stripper and a degreaser. In the food industry, it has been used to decaffeinate coffee and tea as well as to prepare extracts of hops and other flavorings. Its volatility has led to its use as an aerosol spray propellant and as a blowing agent for polyurethane foams.

CHAPTER 3

THEORY

3.1 FORMATION OF PHASE INVERSION-BASED ASYMMETRIC MEMBRANE

Membrane can be prepared by many ways but phase inversion technique is used widely in industry. Phase inversion refers to the process by which a polymer solution inverts into a swollen three-dimensional macro molecular network or gel (Kesting, 1985). This process involves the inversion of liquid homogenous polymer solution into a two-phase system with a solid, polymer-rich phase forming the rigid membrane structure and a liquid, polymer-lean phase forming membrane pores. It dictates the morphology of final membrane, which, in turn, governs the characteristic transport properties of the membranes such as flux and selectivity or rejection. The skin (the uppermost surface) structure and cross-sectional morphology of the asymmetric membranes strongly depend upon the thermodynamics and kinetics of the phase inversion process. There are three techniques in phase inversion which are thermal process, dry or complete evaporation process and wet or combined evaporation-diffusion process.

Membranes obtained by phase inversion can be classified as homogeneous (symmetric) or asymmetric membrane. Asymmetric membranes consist of an extremely thin layer (skin or active layer) on the top of a more or less porous sublayer. In this technique, a polymer solution is immersed in a non-solvent (coagulant) bath and solvent–non-solvent exchange will occur between the polymer solution and the non-solvent. This exchange forms the nascent pores. Depending on the formation conditions, a variety of different morphologies can be prepared as will be discussed later. Traditionally, casting dopes are ternary polymer solutions, containing a mixture of polymer(s), solvent(s), and non-solvent (Wienk, 1995).

Phase separation is a process in which an initially homogenous casting solution becomes thermodynamically unstable due to external effects (Yip and McHugh, 2006). Phase separation of casting solution can be induced by four different techniques;

a) Polymer precipitation by solvent evaporation

This is one of the earliest methods of making microporous asymmetric membrane (Baker, 2004). A polymer is dissolved into a two-component solution mixture consisting of a volatile solvent such as acetone and less volatile non-solvent typically water or alcohol. The solution is then cast onto a glass plate. The volatile solvent is allowed to evaporate at certain period of times so the casting solution is enriched with the less volatile non-solvent. The non-solvent enriched casting solution will precipitate to form the membrane structure.

There are many factors that affect the porosity and pore size of membrane formed through this method. Fine pores membrane will be formed for a short evaporation time. Larger pores membrane is produced if the evaporation step is prolonged. Porosity is mainly affected by non-solvent composition of the casting solution. Increasing non-solvent composition will increase the porosity of membrane and vice versa (Ruthven, 1997).

b) Thermal precipitation

This is the simplest method to fabricate asymmetric membrane. A prepared film is cast from a hot, one – phase polymer solution, followed by cooling to precipitate the polymer. The cooled film is separated into two phase region; polymer-matrix phase and membrane pore-phase. The initial composition of the polymer solution will determine the pore volume of final membrane but the cooling rate of the solution greatly influences the pore size of the final membrane. Rapid cooling will produce small pores (Ruthven, 1997).

c) Polymer precipitation by Absorption of Water Vapor

In this technique, water vapor is required to induce phase separation during membrane fabrication process. The casting solution that consists of polymer, volatile solvent and non-volatile solvent is cast onto a continuous stainless steel belt. The cast film is passed along the belt through a series of chambers. During circulation, the film loses the volatile solvent by evaporation and simultaneously absorbs water vapor from the atmosphere. After precipitation, the membranes are passed into an oven to dry the remaining solvent. The membrane formed is usually used for microfiltration purpose (Baker, 2004).

d) Polymer precipitation by immersion in a non-solvent bath

In this method, casting solution is cast onto glass plate and then immersed into precipitation bath typically water bath. Dense, permselective skin layer is formed by the presence of water. Water will precipitate the top surface of cast solution rapidly. This dense surface will slow down the entry of water into underlying polymer solution so precipitation process is slower. The membrane produced from this method consists of two layers, which are first layer for dense skin surface and second layer for porous support. The dense skin varies from 0.1-10 μ m thick (Ruthven, 1997).

3.2 TERNARY PHASE DIAGRAM

A ternary diagram is used for describing the phase separation process of a system composed of polymer/solvent/coagulant. In this diagram the equilibrium curve known as the binodal curve, divides the area of the triangle into the 2 following regions. One-phase region: every composition of solvent/ polymer/coagulant in this region forms a homogeneous one-phase solution. It is obvious that the dope composition must lie in this region. Two-phase region: every composition of solvent/polymer/coagulant in this region separates into two equilibrium rich and lean polymer phases whose compositions are given by the two ends of the tie lines.

On the other hand, the spinodal curve represents the curve where all possible fluctuations lead to phase separation (Machado, *et al*, 1999). The region between the binodal and spinodal curves implies metastable compositions where phase separation by nucleation and growth takes place. As has been shown in Fig. 1, the intersection point of these two curves is defined as the critical point (C).

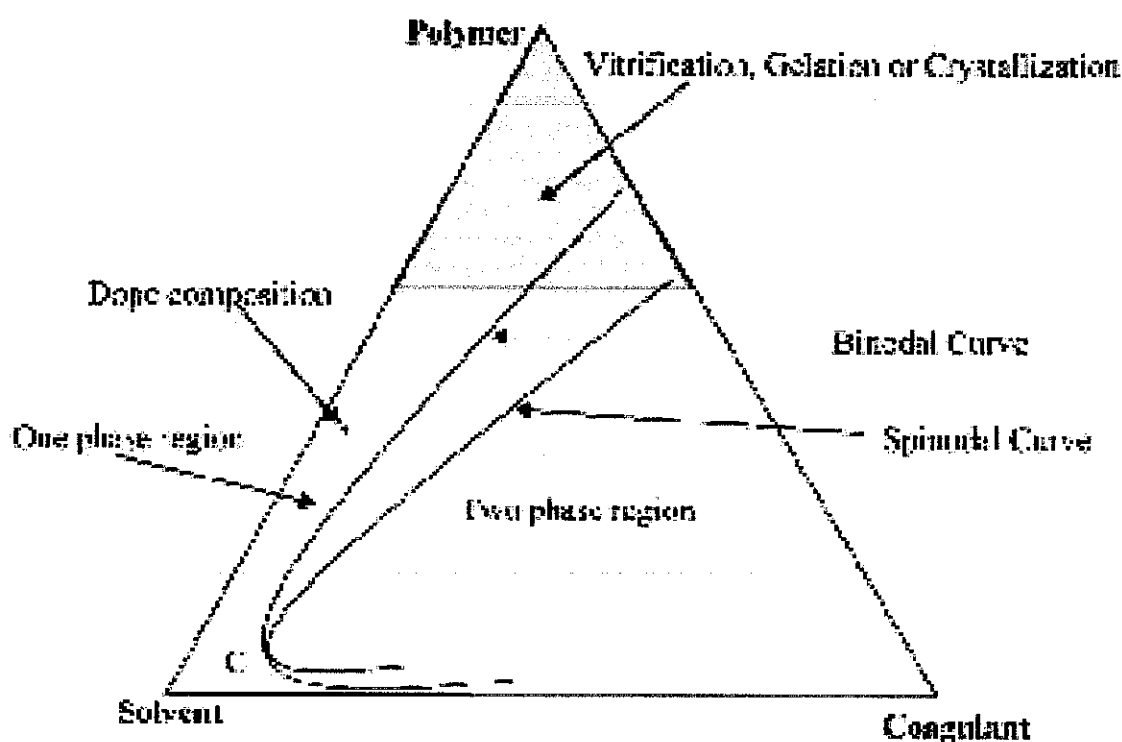


Figure 3.1 Schematic Phase Diagram

The morphology and properties of the membrane are strongly related to the dope position, critical point position and precipitation path. If the precipitation path crosses the binodal curve, phase separation starts with nucleation and growth of the polymer-rich or polymer-lean phase (Albrecht, 2001). Usually when the polymer concentration is low, the precipitation path crosses the equilibrium line below the critical point and nucleation of a polymer-rich phase initiates the phase separation process. But when the polymer concentration is high, the mentioned path passes through the binodal curve above the critical point. In this case, nucleation of the polymer-lean phase may occur. On the other hand at high polymer concentrations, the precipitation path bypasses the binodal curve and

phenomena such as vitrification, gelation or crystallization will occur without polymer-lean phase growth.

In addition to the precipitation path and the mechanism for membrane formation, the time of phase separation initiation after immersion is very important in order to predict the morphology and separation properties of the resulting membrane. If precipitation is initiated immediately after immersion (instantaneous demixing), the resulting membranes have a porous top layer and if precipitation begins after measurable time (delayed demixing) one can expect a membrane with a dense skin layer. (Mulder, 1996). Therefore, the membrane formation path and the demixing process are in initial parameters that can affect skin layer formation of asymmetric membranes (Han, 1999). That is, by changing the demixing time and the precipitation path during membrane preparation one can improve the membrane morphology and separation property.

3.3 PREDICTION OF SOLUBILITY PARAMETER

Solubility parameter is associated to the cohesive energy-density (CED), which is a measure of the strength of secondary bond (Rodriguez, *et al.*, 2003). Secondary bond of a molecule determines most of the physical properties such as boiling point or melting point. While dissolving, melting, vaporizing, diffusion and deformation involve the making and breaking of the secondary bond (Rodriguez, *et al.*, 2003). The solubility parameter is formulated as follows:

$$\delta_i = \sqrt{CED} = \sqrt{\frac{\Delta E_i^V}{V_i}} \quad (3.1)$$

where ΔE_i^V is defined as the energy change upon isothermal vaporization of the saturated liquid to the ideal gas state at infinite dilution and V_i is the molar volume of the liquid (Rodriguez, *et al.*, 2003). Eq (3.1) can be used to predict the solubility parameter of a pure solvent but it is not possible to calculate the solubility parameter of solid polymer since vaporization does not occur in solid polymers. Therefore, the solubility parameter of a polymer can be determined indirectly using a method called group - contribution method. The

calculation of solubility parameter, δ_1 , using group contribution method requires a molar attraction constant, F_i , for each chemical group in the polymer repeating unit. The calculation of solubility parameter using group-contribution method is given as follow (Ebewele, 2000):

$$\delta_i = \frac{\rho \sum_{i=1} F_i}{M_{r_i}} \quad (3.2)$$

in which M_r and ρ refer to the molecular weight and density of polymer, respectively. There are numerous group-contribution methods proposed by several scientists such as those given by Small, Hoy and Van Krevelen (Dijk and Wakker, 1997). Some molar attraction constant, F_i , of chemical groups that are not available in one method can be encountered in another method. For example, the value of molar attraction constant for nitrate is mentioned in Small's method but not in Hoy and Van Krevelen's method (Dijk and Wakker, 1997).

Even though numerous methods have been proposed to predict the interaction between a polymer and a solvent, the prediction is less accurate if hydrogen bondings exist in the molecule structure of polymer or solvent. Therefore, to improve prediction of solubility parameter either for polymer or solvent, a three-dimensional solubility parameter, as proposed by Hansen can be used. The overall solubility parameter is expressed as follows (Hansen, 2000; Krevelen, 1990):

$$\delta = \sqrt{\delta_d^2 + \delta_p^2 + \delta_h^2} \quad (3.3)$$

where δ_d , δ_p , δ_h are the dispersive, polar and hydrogen-bonding solubility parameters, respectively. The magnitude of δ_d , δ_p , δ_h are known to exist for limited numbers of solvent only. Therefore, a prediction to predict these quantities is noteworthy. Hoftyzer and Van Krevelen have developed an approach to calculate those solubility parameters (Krevelen, 1990). They derived a few equations in order to get the magnitude of each solubility parameters. Those equations are presented as follow:

$$\delta_d = \frac{\sum F_{di}}{V}, \quad \delta_p = \frac{\sqrt{\sum F_{pi}^2}}{V} \text{ and } \delta_h = \frac{\sqrt{\sum E_{hi}}}{V} \quad (3.4)$$

The group contributions of F_{di} , F_{pi} and E_{hi} are well-documented by Van Kravlen and Hoftyzer (Krevelen, 1990).

The interaction among all components involved in casting solution is represented by the solubility parameter difference. In Hansen solubility parameter, there are three components that determine the overall solubility parameter. Therefore, solubility parameter difference among all constituents in casting solution cannot simply be calculated as shown in Eq (3.5). Each component of Hansen solubility parameter must be taken into consideration. Hence, solubility parameter difference may be calculated according to the following equation (Chun, *et al.*, 2000):

$$\Delta\delta = \sqrt{(\delta_{i,d} - \delta_{j,d})^2 + (\delta_{i,p} - \delta_{j,p})^2 + (\delta_{i,h} - \delta_{j,h})^2} \quad (3.5)$$

Casting solution may be constituted from many components of solvents or non-solvents. The effective of Hansen solubility parameter of this mixture may be predicted according to the following equation (Barton, 1995):

$$\delta_i^2 = \sum \delta_d^i \phi^i + \sum \delta_p^i \phi^i + \sum \delta_h^i \phi^i \quad (3.6) \quad \text{where}$$

δ^i is the solubility parameter and ϕ^i is volume fraction of i species.

CHAPTER 4

METHODOLOGY

4.1 COAGULATION VALUE DETERMINATION

Material: Polysulfone UDEL P-1800 was purchased from Solvay Advanced Polymer, Ethanol from HmbG Chemicals [molecular weight= 46.07 g/mol; SG=0.7906], Water, NMP from Merck Schuchardt [molecular weight= 99.13 g/mol; SG= 1.031-1.033], and DCM from Merck kGaA [SG= 1.324-1.326]. All reagents were used without any further purification.

Table 4.1 Sample Compositions of Polymer Solutions

Chemical	SG	Volume/Mass			
		NMP 100w%	NMP 75 w% / DCM 25 w%	NMP 50w% / DCM 50 w%	DCM 100 w%
PSF, g	1.24	1	1	1	1
NMP, ml	1.031-1.033	47.53	35.65	23.76	-
DCM, ml	1.324-1.326	-	9.25	18.50	37.01

Note: SG values are provided by the suppliers of each chemical. Lower SG is used for values in range.

1g PSF is added into 49g solvents (DCM or NMP) in an airtight bottle. The polymer solution was stirred using a magnetic stirrer until the PSF powder totally dissolved. The non-solvent mixture which contains 50w% water and 50w% ethanol is slowly titrated into this homogenous solution while stirring until the clear polymer solution becomes turbid or cloudy visually. The point where the solution becomes turbid is referred to as the cloud point. The solution composition at the cloud point is will be computed from the amount of polymer, solvent, and non solvent present in the beaker. A phase diagram can be obtained from a series of the cloud points observed.

4.2 MEMBRANE FABRICATION

4.2.1 Experimental

Membranes are prepared from Polysulfone (P-1800, Solvay Advanced Polymer. This polymer is soluble in several common organic solvents. Dichloromethane and N-Methylpyrrolidone. Both solvents will be used as the solvent while water and ethanol will be the coagulants. The weight percentage of coagulants will be fixed. The focus will be on the different solvents used.

The compositions of the four casting solutions are as follow;

- 1) 15 w% PSF, 85 w% NMP
- 2) 15 w% PSF, 63.75 w% NMP, 21.25 w% DCM
- 3) 15 w% PSF, 42.5 w% NMP, 42.5 w% DCM
- 4) 15 w% PSF, 85 w% DCM

The composition of the coagulant is being fixed for all cast solution which is 50w% water and 50w% ethanol. Below is the calculation for the volume/mass of each component in each cast solution.

Table 4.2 Membrane Fabrication Calculation

Chemical	SG	Volume/Mass			
		NMP 100w%	NMP 75 w% / DCM 25 w%	NMP 50w% / DCM 50 w%	DCM 100 w%
PSF (g)	1.24	7.5	7.5	7.5	7.5
NMP (ml)	1.031-1.033	41.22	30.92	20.61	-
DCM (ml)	1.324-1.326	-	8.02	16.05	32.1
Ethanol	0.7906	50 w% each			
Water	1				

Note: SG values are provided by the suppliers of each chemical. Lower SG is used for values in range.

15w% polymer and 85w% solvent will be blended together. Polysulfone is dried for 24 hours in the oven at 100°C prior to use. The solvent contains DCM (dichloromethane) or NMP (N-methyl pyrrolidone) or the combination of both. (Refer to Table 4.2). The percentage for non-solvent used in coagulation bath is 50w% water and 50w% ethanol.

The solvents and the polymer are mixed together in a beaker and stirred on the hot plate at 35°C for 24 hours. Airtight bottle is preferably used in order to avoid any evaporation while stirring because the mixtures are volatile or otherwise aluminium foil can be used to cover the beaker. Powder adding which is PSF should be done slowly to make sure it disperses well into the solution.

The mixed solution is put in the sonification bath for four hours to remove the bubbles. The solution will be flattened or spread on the glass plate by the casting knife manually at 500µm thickness setting.

Coagulation medium is prepared with water and ethanol as coagulant with 50w% each. The glass plate is soaked slowly in the coagulation bath to allow the phase inversion to occur. To ensure the phases exchange process is complete, the glass plate is immersed for two hours in the coagulation bath. Membrane will de-attach itself from the glass plate within sometimes. The membrane is then washed with deionized water and air-dried before testing.

4.3 MEMBRANE CHARACTERIZATION

4.3.1 Scanning Electron Microscopy (SEM)

Scanning electron microscopy was used to characterize the structure of surface and sub-layer of membrane. Images obtained from SEM shows detailed 3-dimensional at much higher magnifications than is possible with a light microscope. Magnification of images is created by electrons instead of light waves as in conventional light microscope, which uses a series of glass lenses to bend the light waves.

Membrane structure was determined by LEO 1430 VPSEM. Cross-section of the PSf membranes were chosen randomly and then was cut carefully using a sharpened razor blade. Samples were then coated with gold using a sputter coater. After coating, membrane samples were observed using SEM with magnification range from 600 to 1000 X.

4.3.2 Porosity Calculation

Membrane porosity or void fraction, ε , was calculated from the thickness, l , area of the membrane, A , and the weight of samples, m . Thickness was determined directly from scanning electron microscopy (SEM). As a result, the overall porosity can be calculated as follows (Jansen *et al.*, 2005; Chun *et al.*, 2000)

$$\varepsilon = \frac{V_{void}}{V_{tot}} = \frac{lA - (m / \rho)_{pol}}{lA} \quad (4.1)$$

in which V_{void} and V_{tot} are the void volume and the total volume of membrane. Polymer density is denoted with ρ . Polysulfone has density of 1.24 g/cm³ as presented in Appendix A, Table A.1.

4.3.3 Gas Permeation Studies

Gas permeation measurements were performed using pure CO₂ and pure CH₄. The permeation experiment always begin with nitrogen and ended with carbon dioxide. Feed side pressure was varied from 1 bar to 5 bar. The set-up consists of a feed gas tank, a pressure gauge of inlet gas, a dead-end membrane cell and a bubble soap flow meter. Membranes were located in the dead end membrane cell or module. This type of module allows the feed gas to flow into the membrane perpendicularly to the membrane position.

Before performing the experiment, the gas permeation test unit was evacuated to less than 0.1 bar by vacuum pump for 1 hour to remove all residual gases remaining in the equipment. The feed gas was supplied directly from the gas tank, which is equipped with a pressure regulator. The feed gas pressure was set up within range of test pressure and the permeate stream was assumed to be at atmospheric pressure. In this permeation experiment, time (t) required to reach certain volume of gas in the permeate stream was observed and recorded. In addition, the volume of gas (V) in permeate stream was also measured using a bubble soap flow meter. The permeation of each gas through a membrane was measured twice at steady state condition.

Based on the volumetric measurements of the permeated gas, the volumetric flow rate, Q , was calculated as follows :

$$Q = \frac{V}{t} \quad (4.2)$$

This volumetric flow rate was then corrected to STP conditions (0°C and 1 atm) using the following equation

$$Q_{STP} = \frac{T_{STP}}{T} \times Q \quad (4.3)$$

in which T_{STP} and Q_{STP} referred to temperature (K) and volumetric of permeate gas (cm^3/s) at STP condition. After conversion into STP condition, gas permeance, $\frac{P}{l}$, was then calculated using the following formula

$$\frac{P}{l} = \frac{Q_{stp}}{A \times \Delta p} \quad (4.4)$$

where Δp and A were trans-membrane pressure and effective membrane area, respectively. The CO_2/CH_4 ideal selectivity (unitless), $\alpha_{\text{CO}_2/\text{CH}_4}$, of asymmetric membrane can be determined by dividing CO_2 permeance, $(P/l)_{\text{CO}_2}$, over CH_4 permeance, $(P/l)_{\text{CH}_4}$.

$$\alpha_{\text{CO}_2/\text{CH}_4} = \frac{(P/l)_{\text{CO}_2}}{(P/l)_{\text{CH}_4}} \quad (4.5)$$

4.3.4 Molecular Interactions

The most direct to study the nature of a polymer mixture is by using FTIR spectroscopy. The spectra of incompatible polymers are simply the sum of the spectra of the pure polymer components. In the case of miscible blends, frequency shifts usually indicate specific interactions between the characteristic groups of the pure polymer (Koenig, 1992). FTiR-84000S Shimadzu is used to measure the molecular interactions between the polymer blends of different concentration.

4.3.5 Mechanical Properties

Mechanical properties of the membrane samples were determined by ASTM D882-02 standard test method for tensile properties using universal testing machine (UTM) LR 5K Lloyd Instruments. For each membrane, 100mm x 10mm was prepared and tested to keep constancy.

Universal Testing Machine (UTM) is used to test the tensile and compressive properties of materials. Tensile properties include the resistance of materials to pull or stretch forces. The amount of force required to break a material and the amount it extends before breaking are important properties. Analysis of force elongation or stress-strain curves can convey much about the material being tested, and it can help in predicting its behavior.

The stress and strain can be calculated using the following formula:

$$\sigma_e = \frac{P}{A_0}, \quad \epsilon_e = \frac{\delta}{L_0}$$

The engineering measures stress (σ_e) and strain (ϵ_e) are determined from the measured the load and deflection using the original specimen cross-sectional area A_0 and length L_0 .

4.4 TOOLS AND EQUIPMENT

4.4.1 Lab tools and equipments for membrane fabrication;

Beakers, spatula, testing tubes, aluminium foil, airtight bottles, coagulation bath, casting knife, glass plate, magnetic stirrer, hot plate, balance, measuring cylinders.

4.4.2 Equipments for characterization;

1. FTIR to measure molecular interactions
2. SEM to analyse the morphology
3. UTM to measure the mechanical properties
4. Gas permeation cell to evaluate the performance of membrane by applying different feed pressure

4.5 KEY MILESTONES

Table 4.3 Key Milestones

No	Action Item	Action By	Note
1.	Briefing & update on students progress	Coordinator / Students / Supervisors	WEEK 1
2.	Project work commences	Students	WEEK 2 -4
3.	Submission of Progress Report 1	Students	WEEK 5
4.	Submission of Progress Report 1 Marks	Supervisors / FYP Committee	WEEK 6
5.	Submission of Progress Report 2 (Draft of Final Report)	Students	WEEK 11
6.	Poster Exhibition / Pre-EDX/ Progress Reporting	Students / Coordinator	WEEK 11
7.	EDX	Selected Students/ Coordinator	WEEK 12
8.	Submission of Final Report (CD Softcopy & Softbound)	Students / Supervisors	WEEK 14
9.	Delivery of Final Report to External Examiner / Marking by External Examiner	FYP Committee / Coordinator	WEEK 15
10.	Final Oral Presentation	Students/ Supervisors / Internal & External Examiners/ FYP Committee	WEEK 18 - 19
11.	Submission of hardbound copies	Students	WEEK 20

4.6 GANTT CHART

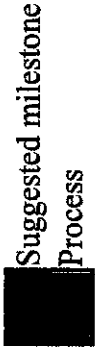
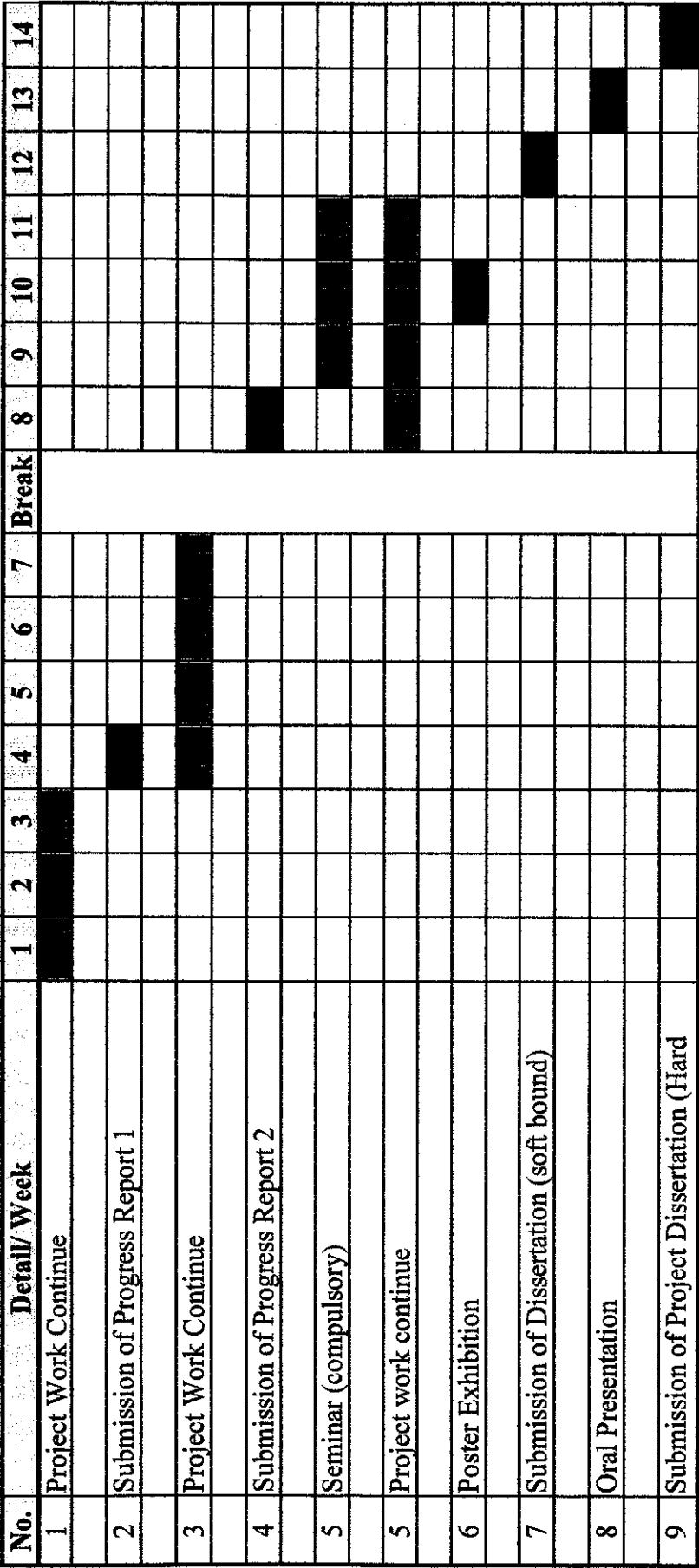


Figure 4.1 Gantt Chart

CHAPTER 5

RESULT AND DISCUSSION

5.1 FORMATION AND MORPHOLOGIES OF ASYMMETRIC PSF MEMBRANE

Asymmetric Polysulfone (PSF) membrane formation and morphologies at different solvent mixtures are presented in this section. Formation of macrovoid in the substructure and overall porosity of the membrane as result of the different concentration of solvents are also discussed.

5.1.1 Effect of Solvents

Solvent selection plays an important role in controlling the membrane morphologies and properties. Figure 5.1 shows the SEM images of cross-section of asymmetric PSF membrane prepared from various solvent type and concentration. Result from SEM images shows that asymmetric PSF membrane were successfully produced using NMP and DCM as solvents at different concentrations. All of these fabricated membranes are composed of skin layer supported with closed-cell substructure. However, various solvents used produced different membrane morphologies in term of porosity and macrovoid substructure.

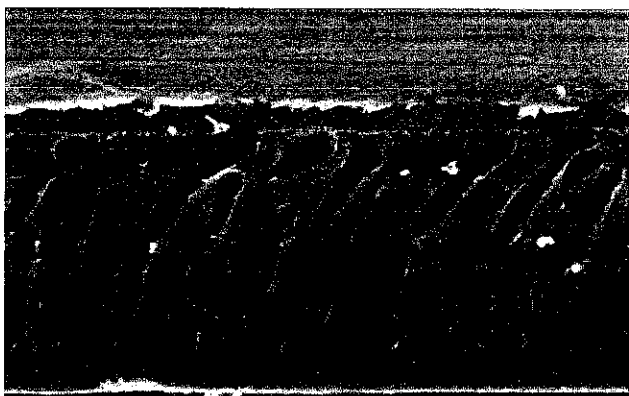


Figure 5.1 (a) SEM image for NMP 100w%



Figure 5.1 (b) SEM image for
NMP 75w% / DCM 25w%

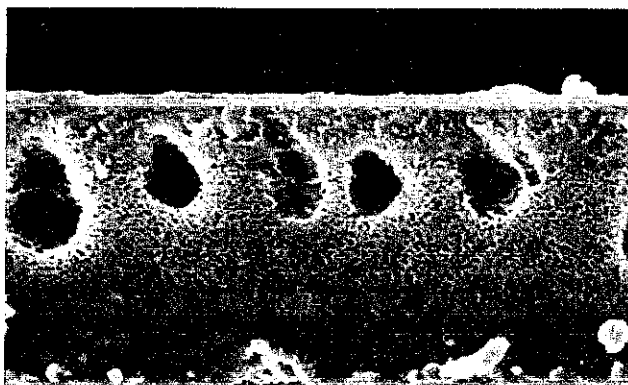


Figure 5.1 (c) SEM image for NMP 50w% / DCM 50w%



Figure 5.1 (d) SEM image for DCM 100w%

A distinct layer region on the top side of the membranes can be observed distinctly on NMP 100 w% and NMP 75 w%/DCM 25 w% membranes. On the contrary, less distinct skin layer region was obtained for NMP 50w%/DCM 50w% and DCM 100w% membranes. Almost no pores can be seen on DCM 100 w% membrane with SEM within 600-1000 focus range. The morphology of NMP 50w%/DCM 50w% and 85% DCM membrane were also characterized by lower porosity and less macrovoid substructure while both NMP 100 w% and NMP 75 w%/DCM 25 w% membranes have higher porosity and more macrovoid substructure. A comparison of the porosity of asymmetric PSF membranes prepared using NMP and DCM can be observed in Table 5.1.

Table 5.1 Membranes porosity prepared using different solvent mixture.

Solvents	Membrane Thickness (μm)	Porosity, (%)
NMP 100w%	91.27	59.11
NMP 75w%/DCM 25w%	69.78	58.39
NMP 50w%/DCM 50w%	54.57	56.08
DCM 100%	40.05	43.62

Table 5.1 shows that high DCM concentration membrane has less porous substructure than that of the high NMP concentration. The membrane thickness measured using SEM might be smaller than the actual measurement because the overall thickness of the membrane might be compressed when they were cut using razor blade during SEM sample preparation.

In order to study the mechanism of asymmetric membrane fabrication prepared by wet phase inversion method, the effect of immersion precipitation step on the change of membrane structure must be considered. Miscibility or affinity among all the constituents involved during fabrication is necessary to be taken into account in determining the morphology of membrane. Affinity between solvent and polysulfone as well as solvent and coagulant can be expressed quantitatively through solubility parameter difference. Various solvent used in membrane making process would affect the solubility parameter of casting solution. The solubility parameter for each component involved in the membrane making process in this work is presented in Appendix B, Table B.1. In membrane making process through wet phase inversion method, the polymer must be dissolved into solvents. In this work, NMP and DCM were used as solvent for polysulfone. Accordingly, the solubility parameter of the solvent and coagulant mixtures must be also taken into account in expressing the interaction between solvent and polymer as well as solvent and coagulant. The calculated solubility parameter is tabulated in Table 5.2.

Table 5.2 Solubility parameter of PSf, solvents and coagulant mixtures.

Component	δ_d (Mpa) ^{1/2}	δ_p (Mpa) ^{1/2}	δ_h (Mpa) ^{1/2}	δ_{mix} (Mpa) ^{1/2}
PSf	21.5	2.8	6.8	22.7229
NMP 100w%	18	12.3	7.2	22.9593
NMP 75w%/DCM 25w%	18.0412	11.0635	6.97332	22.2826
NMP 50w%/DCM 50w%	18.0876	9.67325	6.71843	21.584
DCM 100%	18.2	6.3	6.1	20.2025
Water/Ethanol	15.6675	11.979	29.511	35.4946

From Table 5.2, it can be observed that solubility parameter of NMP based solvent is larger than that of NMP 75w%/DCM 25w%, NMP 50w%/DCM 50w% and DCM. Consequently, each solvent has different interaction with polysulfone and coagulant. The solubility parameter difference between solvent and coagulant mixture, $\Delta\delta_{(s-c)}$, as well as solvent and polysulfone, $\Delta\delta_{(s-PSf)}$, are presented in Figure 5.2.

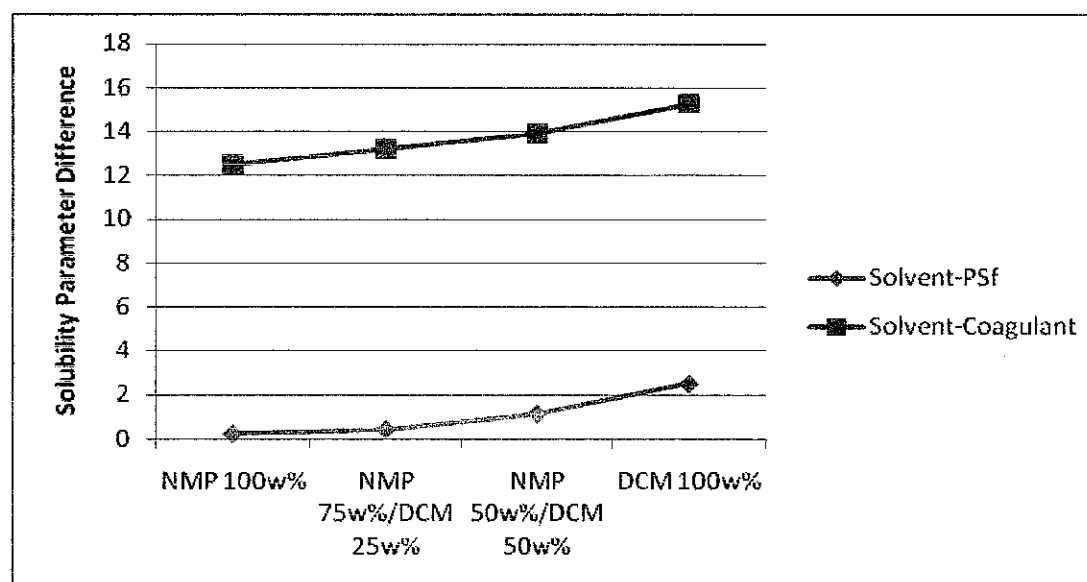


Figure 5.2 Solubility parameter difference between solvent to coagulant, $\Delta\delta_{(s-c)}$, and solvent to polysulfone, $\Delta\delta_{(s-PSf)}$.

As presented in Figure 5.2 each solvent system has different solubility parameter difference with coagulant, and PSf, $\Delta\delta_{(s-PSf)}$. NMP solvent has higher total solubility parameter than the other solvent mixtures. Thus, solubility parameter difference between NMP based solvent with coagulant $\Delta\delta_{(s-c)}$, is smaller than the other systems. This indicates that the NMP solvent

is more miscible to coagulant mixture than other solvent mixtures. The solvents in the order of increasing solubility parameter difference between casting solution to coagulant are NMP 100w% < NMP 75w%/DCM 25w% < NMP 50w%/DCM 50w% < DCM 100w%.

Various solvents could also affect the solubility parameter difference between solvent and PSf, $\Delta\delta_{(s-PSf)}$, as presented in Figure 5.2. Smaller solubility parameter difference between NMP solvent and polysulfone, $\Delta\delta_{(s-PSF)}$ makes it the most miscible solvent to polymer. The miscibility of polysulfone with solvent mixtures decreased in the order of NMP 100w% > NMP 75w%/DCM 25w% > NMP 50w%/DCM 50w% > DCM 100w%.

Theoretically, the smaller solubility parameter difference of NMP solvent with polysulfone, $\Delta\delta_{(s-PSF)}$, the more time is needed to remove solvent from the polymer structure. Accordingly, delayed demixing will occur when the casting solution is immersed into coagulation bath to produce less porous (Strathmann and Kock, 1977). This is because, in delayed demixing mechanism, polymer-rich phase of casting film tend to agglomerate before it was solidified to form a membrane matrix (Strathmann, 1975; Baker, 2004). However, as shown in the SEM images (Figure 5.1(a) and Figure 5.1(b)) and porosity calculation, Table 5.1, high NMP concentration-based membrane shows higher porosity even though it has smaller $\Delta\delta_{(s-PSF)}$. This shows that mechanism of membrane formation cannot just be explained using solubility parameter difference of solvent and PSF.

The tendency to form less porous structure could also be driven by the change of solubility parameter difference between solvent mixtures and coagulant, $\Delta\delta_{(s-c)}$. Larger solubility parameter difference of DCM solvent with coagulant should induce the formation of less porous structure due to delayed demixing mechanism. On contrary, smaller solubility parameter difference of NMP-based solvent mixtures and coagulant should induce the formation of more porous structure of membrane via instantaneous demixing mechanism. The effect of solvents on membrane porosity was also investigated by comparing the porosity of the membranes fabricated with DCM and NMP as solvents. In order to further verify the effect of various solvents on the demixing rate of casting solution, the coagulation value and solubility parameter difference of the solvent mixture-coagulant are plotted as in Figure 5.3 for all solvent systems.

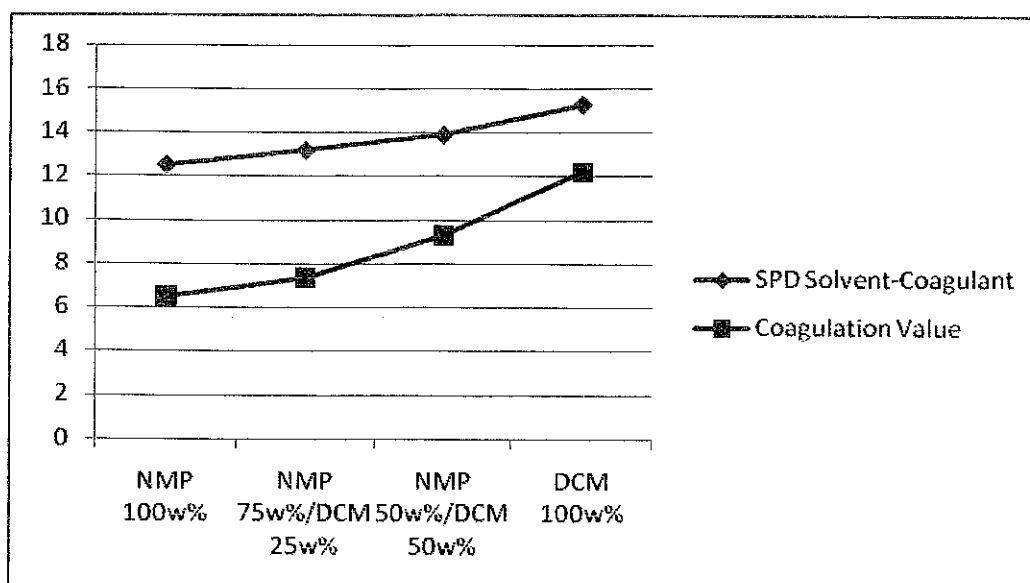


Figure 5.3 Coagulation value and solubility parameter difference of solvent mixtures and coagulant.

According to Figure 5.3, smaller solubility parameter difference of solvent mixture and coagulant correlates to lower coagulation value. Coagulation value indicates the tolerance of a homogenous casting solution on the addition of coagulant (Wang *et al.*, 1995). It refers to the exchange rate between solvent and coagulant during immersion step (Wang *et al.*, 1995). Casting solution that can be separated easily is referred as having lower coagulation value and this kind of casting solution will undergo instantaneous demixing to become unstable instantly. Conversely, a more stable homogenous casting solution has higher coagulation value in which delayed demixing mechanism will occur to induce the formation of asymmetric membrane structure.

The casting solution containing higher NMP concentration has smaller coagulation value. Therefore, once it was immersed into coagulation bath, it should demixed instantaneously and subsequently, a more porous substructure should be obtained for membranes prepared from high NMP concentration. Contradictive results were observed in which less porous structure was resulted from DCM-based membrane and a more porous structure was observed on NMP-based membrane as shown in SEM images in Figure 5.1 and porosity calculation in Table 5.1. This phenomenon suggest that the effect of solvent-coagulant interaction is more dominant than solvent-polymer interaction in controlling the mechanism of asymmetric PSF membrane formation. Thus, instead of producing less porous structure due to higher miscibility between polymer and solvent, NMP-based membrane shows more

porous structure with the presence of macrovoid due to higher miscibility between solvent and coagulant and less volatile properties of NMP that could minimize the formation of polymer-concentrated region on the top side of casting film.

5.2 CO₂/CH₄ SEPARATION CHARACTERISTIC

All membranes prepared from different solvent mixtures were subjected to the same operating conditions to determine their gas separation characteristic. The feed pressure was varied within 1 bar – 5 bar while temperature is assumed constant at 25°C during experiment.

In this work, to obtain reliable result, two membranes which were prepared under same preparation condition were tested twice in a single gas permeation set-up. Experimental results showed that asymmetric polysulfone membranes prepared from different solvent mixture were reproducible in which relative standard deviation of CO₂ and CH₄ permeance as well as CO₂/CH₄ ideal selectivity is relatively small (less than 6 %) as tabulated in Appendix E.

5.2.1 Effect of Solvents

The gas separation characteristic is determined by plotting the permeance of CO₂, CH₄ and CO₂/CH₄ ideal selectivity of each membrane with respect to feed pressure. The permeance of CO₂ and CH₄ of various solvent mixture membrane are presented in Figure 5.4 and 5.5, respectively.

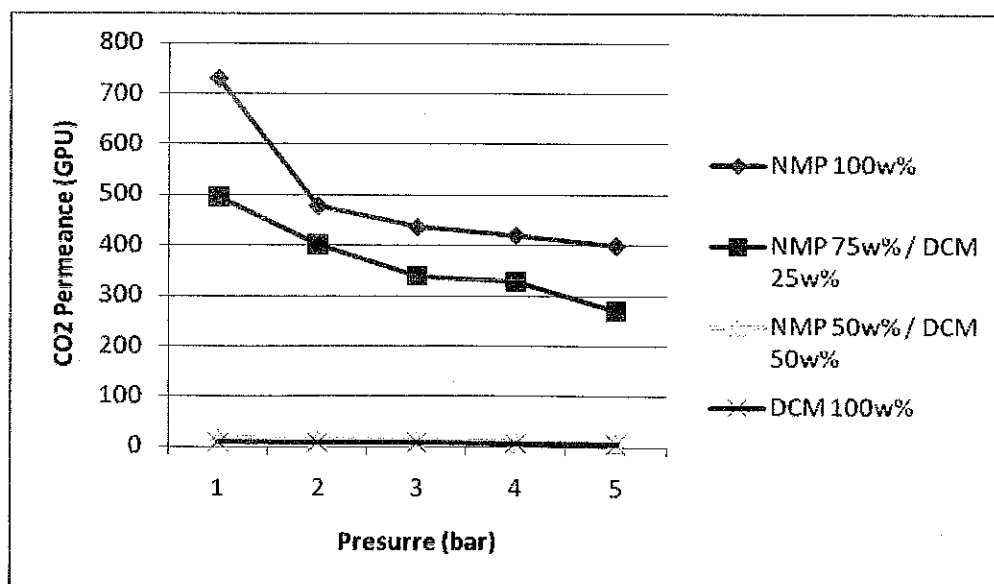


Figure 5.4 CO₂ permeance of membranes prepared from different solvent mixtures at various feed pressures.

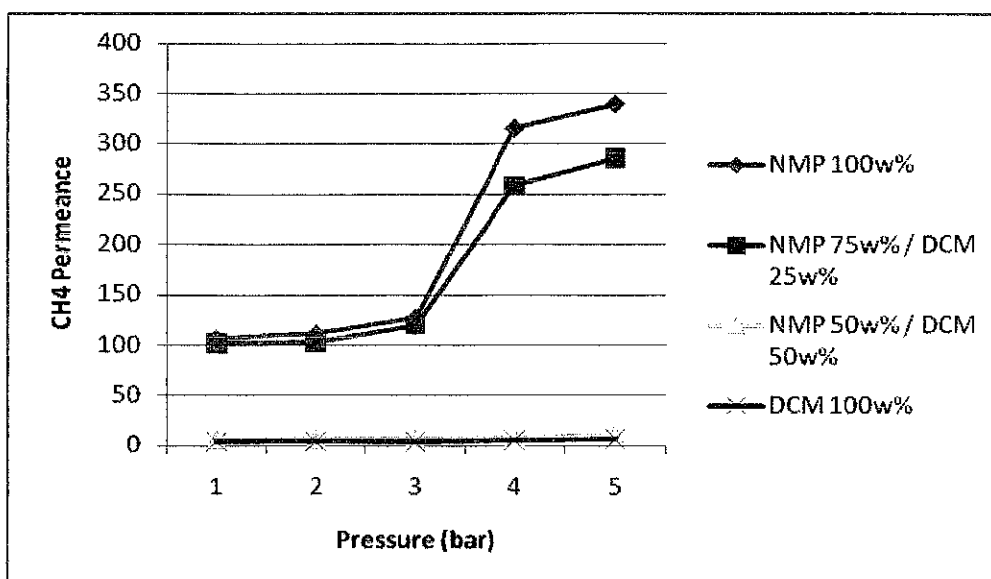


Figure 5.5 CH₄ permeance of membranes prepared from different solvent mixtures at various feed pressure

According to Figure 5.4 and 5.5, CO₂ and CH₄ permeances decrease in the order of NMP 100w% > NMP 75w%/DCM 25w% > NMP 50w%/DCM 50w% > DCM 100w% solvent system. The significant differences of gas permeances among membranes prepared from different solvent mixtures could be explained by referring to their morphologies as shown by SEM images, Figure 5.1. The porosity of substructure played an important role in determining the performance of membrane especially in terms of gas permeance. CO₂ and CH₄ permeances of NMP membrane were higher than the others. This is because NMP membranes have more porous substructure with the presence of macrovoid as compared to DCM membrane. High porosity substructure makes the membrane become less restricted, thus allowing for the sorbed gas to diffuse more easily across the bulk structure of the membrane. While, denser and less porous substructure causes more hindrance for the sorbed gas to diffuse over the entire structure of membrane thus producing lower CO₂ permeance. CO₂/CH₄ ideal selectivity is as shown in Figure 5.6

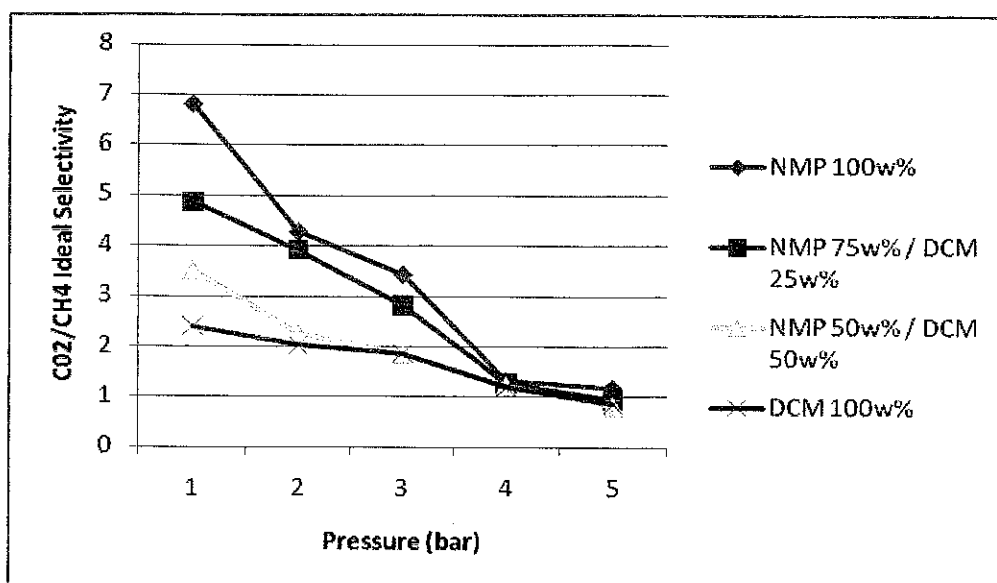


Figure 5.6 CO₂/CH₄ ideal selectivity of membranes prepared from different solvent mixtures at various feed pressures.

NMP membrane yield higher CO₂/CH₄ ideal selectivity as compared to other solvent systems. It indicates that the skin layer of these membranes were homogenously dense and free of defect or pinholes. In all of these membranes, transport mechanism was affected by solution-diffusion mechanism in which polar gas of CO₂ was absorbed more than CH₄. The adsorbed CO₂ would then diffuse through the bulk structure of the membrane to the permeate side. Therefore, CO₂ permeance of asymmetric is always higher compared to CH₄ permeance.

CO₂ permeance of all membranes was also found to decrease as feed pressure increase, Figure 5.4. This is typical behavior of CO₂ transport mechanism through dense membrane due to solution diffusion mechanism as reported by the previous researchers (Koros *et al.*, 1977; Sanders, 1988; Ismail and Lorna, 2002). CH₄ permeance of all membranes increase as feed pressure increase due to increasing of diffusion coefficient of CH₄ (Lin and Chung, 2001).

CO₂/CH₄ ideal selectivity of all membranes decrease as feed pressure increase. The same trend of CO₂/CH₄ ideal selectivity against feed pressure was also reported by Jordan and Koros (1990).

5.3 MOLECULAR INTERACTIONS

All four membranes undergone FTIR test to certify the mixture concentration using FTIR-8400S Shimadzu model. Complete FTIR spectra is attached in Appendix F. Below are the diagrams of FTiR for all membranes.

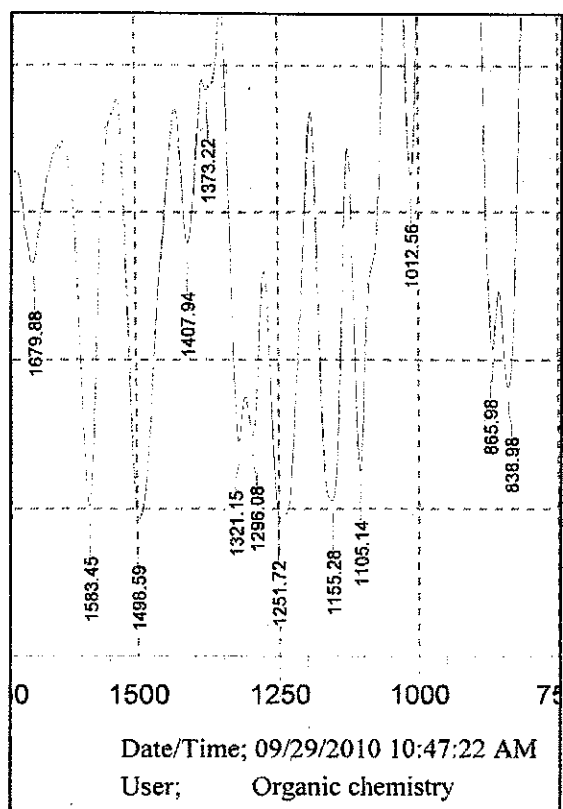


Figure 5.7 (a) FTiR for NMP 100w%

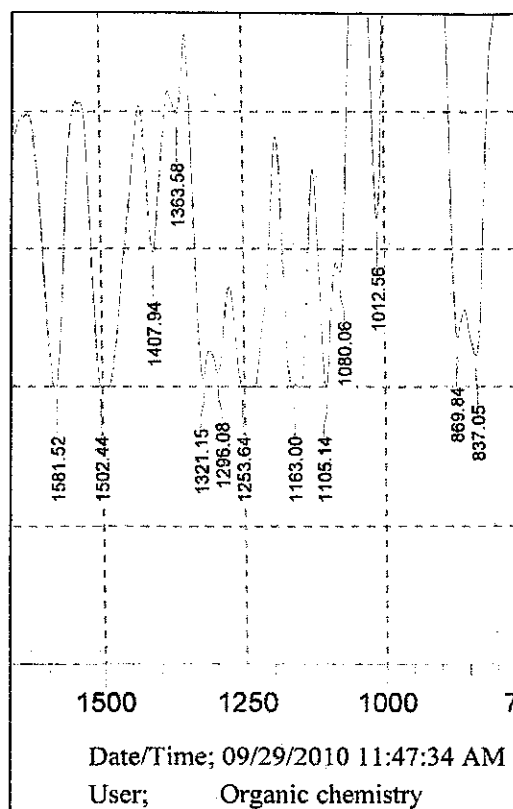


Figure 5.7 (b) FTiR for NMP 75w%/DCM 25w%

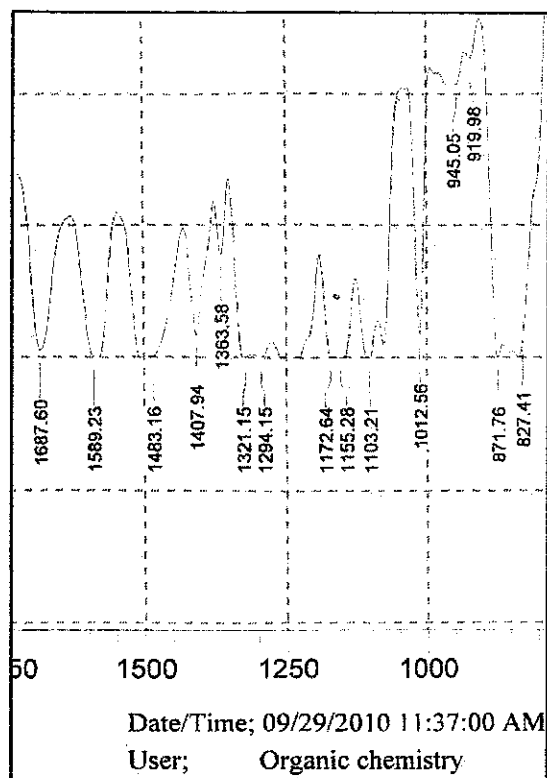


Figure 5.7(c) FTiR for NMP 50w%/
DCM 50w%

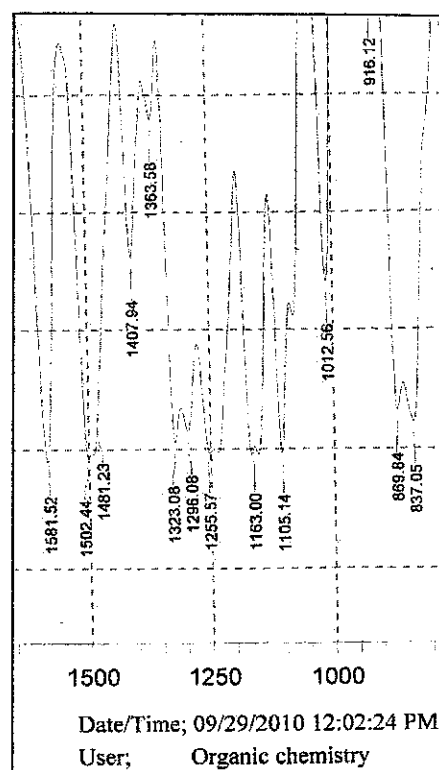


Figure 5.7 (d) FTiR for
DCM 100w%

The sulfonate group of PSF give characteristic peaks at 1155 cm^{-1} . Subtraction of NMP and DCM from NMP/DCM blend spectrum was employed, in order to identify any interactions between the pure components, and their level of mixing compatibility. The strong frequency shifts ($7\text{--}9\text{ cm}^{-1}$) are observed for aliphatic hydrogen vibration (from 1373.22 to 1363.58 cm^{-1}), the sulfonate group of PSF (from 1163 to 1155.28 cm^{-1}) and benzene ring stretching mode (from 1589.23 to 1581.52 cm^{-1}), while secondary shift (3.85 cm^{-1}) is observed for aromatic carbon-oxygen stretching vibration frequency (from 1255.57 to 1251.72 cm^{-1}). These spectra shifts and intensity changes suggest NMP and DCM interactions and mixing at molecular level. Therefore, these structural analysis results support further the compatible nature of NMP/DCM blends membranes indicated by the macroscopic and microscopic observations.

5.4 MECHANICAL STRENGTH

All four membranes were tested according to ASTM D882-02 standard, meant for thin sheet. Based on the diagrams in Appendix F, data of yield strength, Young's Modulus, tensile strength or total elongation can be extracted. The results are tabulated in the table below

Strength of Material	NMP 100 w%	NMP 75w% / DCM 25w%	NMP 50w% / DCM 50w%	DCM 100w%
Tensile at yield (MPa)	387.112	600.989	760.2076	1690.5
Tensile strength (MPa)	400.762	551.063	684.2758	1950.061
Modulus of polymer sample	15825.2	18763.5	59262.79	68948.66

Table 5.3 Strength of Material of Membranes

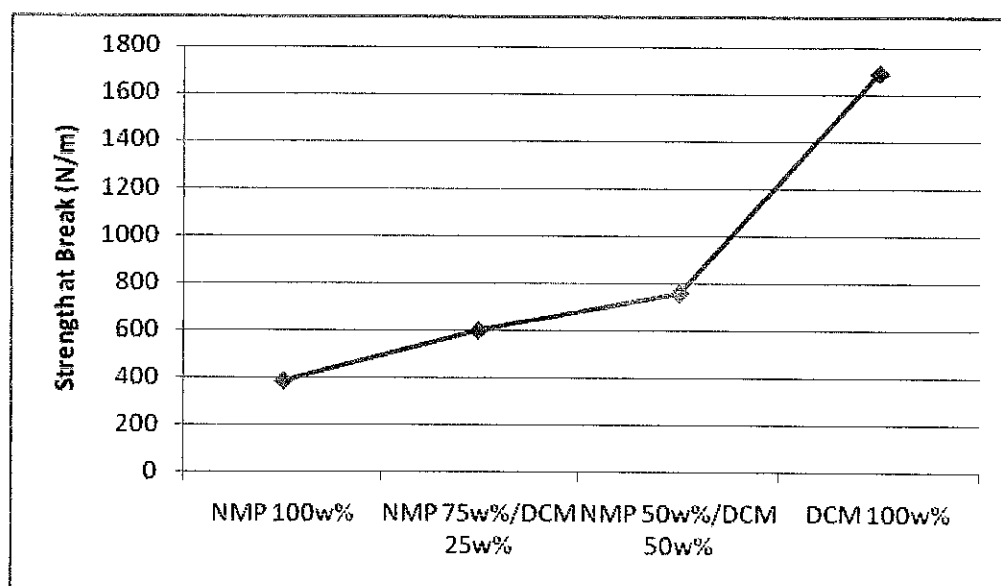


Figure 5.8 Strength at Break (N/m)

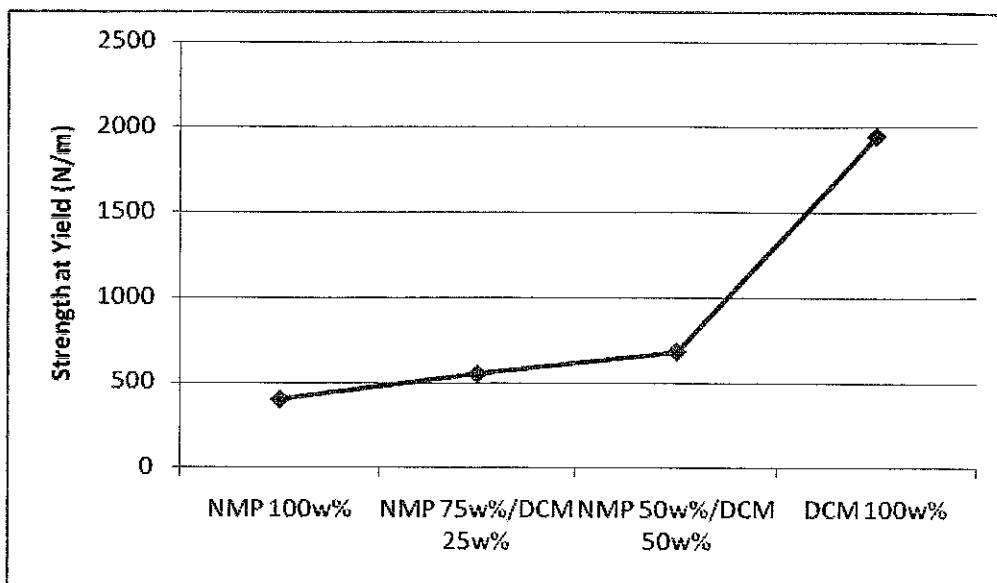


Figure 5.9 Strength at Yield (N/m)

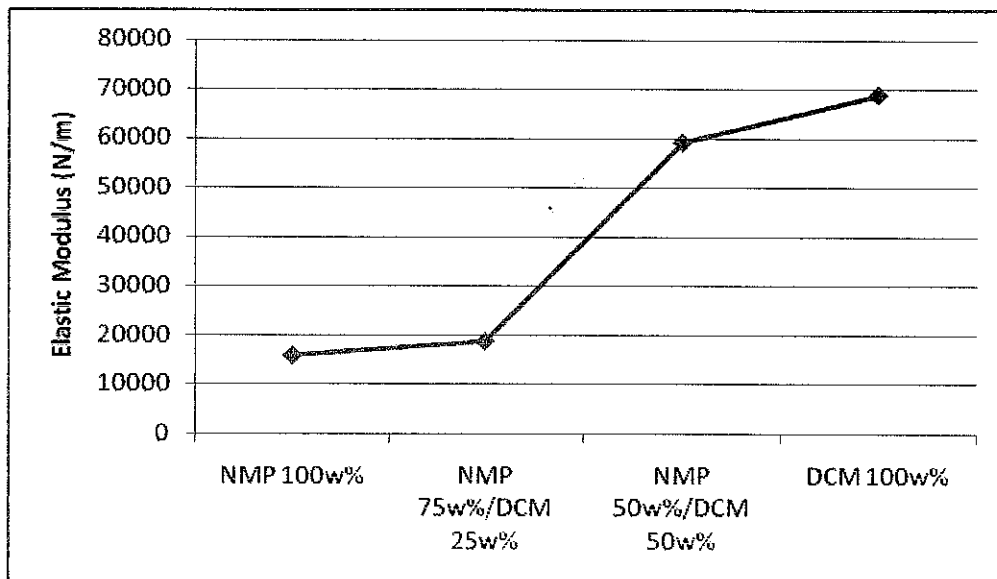


Figure 5.10 Elastic Modulus (N/m)

DCM based membrane has the highest elastic modulus; it will resist deformation for a while, it will eventually deform only after enough stress is applied. It is different from rigid plastic as it doesn't resist deformation and tend not to break. Flexible plastics may not be as strong as rigid ones, but they are a lot tougher. The trend tends to decrease with the increment of NMP composition. NMP based membrane is easier to be broken as shown by its strength at yield or tensile strength. It also has very low strength at break whereby it cannot regain back its initial shape after that much load is applied.

There is significant difference in mechanical strength between polymer made from NMP and DCM. This is due to the presence of the macrovoids in the membrane. NMP based membrane has more macrovoids compared to DCM based membrane. The parameter that leads to the formation of macrovoid is the same as the parameter that leads to the formation of the porous (Mulder, 1996). As we discussed in this chapter earlier, in Section 5.1, NMP based membrane shows more porous according to SEM images and porosity calculation, thus it has more macrovoids. This macrovoids could lower the membrane strength because it provides weak points on the membrane. Therefore, the membrane will be easier to be broken.

CHAPTER 6

CONCLUSION AND RECOMMENDATION

The effect of solvent (NMP and DCM) on asymmetric polysulfone (PSf) membrane on morphology and CO₂/CH₄ separation characteristic have been investigated. Membranes were prepared based on wet phase inversion method. Ethanol and water were selected as coagulation medium.

Asymmetric PSf membrane prepared NMP produced more porous substructure than DCM-based membrane. Overall porosity of membrane in decrease order is NMP 100w% > NMP 75w%/DCM 25w% > NMP 50w%/DCM 50w% > DCM 100w%.

Permeation studies revealed that different morphologies of asymmetric polymeric membrane give significant changes of the membrane performance. It showed that CO₂ and CH₄ permeances of NMP-based membrane were higher as compared to DCM-based membranes. High ideal selectivity of CO₂/CH₄ was obtained for NMP-based membranes which is In these membranes, porosity of substructure played important role in which CO₂ permeance of NMP-based membrane would be higher as compared to other membranes due to high porosity of membrane substructure.

However, the mechanical strength of NMP based membrane is the lowest among the four fabricated membranes. Further studies must be done to produce a good membrane that has both good permselectivity and mechanical strength. Macrovoids has to be avoided but high porosity characteristic must be maintained. Ongoing research is done in incorporating inorganic materials such as carbon molecular sieve (CMS) or fumed silica in order to get the strong and high permselectivity mixed matrix membrane.

APPENDICES

APPENDIX A: RAW MATERIAL PROPERTIES

A.1 Polymer

Table A.1 Properties of Polymer

Polymer	Polysulfone
Manufacturer	Solvay Advanced Polymer
Formula	$(C_{27}H_{22}O_4S)_n$
Characteristic	Odorless
Density (g/cm ³)	1.24
MW (g/mol)	442

A.2 Chemicals

Chemical properties used are presented in Table A.2

Table A.2 List of properties of pure components

Material	Manufacturer	Density (g/cm ³)	MW (g/mol)	Boiling Point (°C)
NMP	Merck Schuchardt	1.031-1.033	99.13	202
DCM	Merck kGaA	1.324-1.326	84.93	40
Ethanol	HmbG Chemicals	0.7906	46.07	78

APPENDIX B: SOLUBILITY PARAMETER

B.1 Solubility Parameter of Pure Components

Table B.1 Solubility parameter of pure components (Hansen, 2000)

Component	$\delta_d(\text{Mpa})^{1/2}$	$\delta_p(\text{Mpa})^{1/2}$	$\delta_h(\text{Mpa})^{1/2}$	$\delta_{\text{total}}(\text{Mpa})^{1/2}$
PSF	21.5	2.8	6.8	22.72
NMP	18.0	12.3	7.2	22.96
DCM	18.2	6.3	6.1	20.20
Ethanol	15.8	8.8	19.4	26.52
Water	15.5	16	42.3	47.81

B.2 Solubility Parameter of Mixtures

Solvent mixtures consist of water/ethanol is used as example to determine overall solubility parameter of solvent mixtures, δ_{mix} . Composition of water/ethanol in mass and density, ρ , of each component are given in Table B.2. Volume, V , for each component can be calculated from known data of ρ and m .

$$V = \frac{m}{\rho}$$

Once total volume of solvent mixtures is obtained, volume fraction, ϕ , can be calculated by dividing volume of component i , V_i , over total volume of solvent mixtures, V .

$$\phi = \frac{V_i}{V}$$

Summary of data calculation for V and ϕ are tabulated in Table B.2

Table B.2 Data tabulation for the total volume, V, and volume fraction, ϕ , of solvent mixtures

	ρ	m (g)	V	ϕ
Water	1.00	250	250	0.44
Ethanol	0.79	250	316.46	0.056
Total			566.46	1

Once the volume fraction of component i , ϕ_i , is obtained, solubility parameter component of solvent mixtures can be calculated as follows:

$$\delta_d = \delta_d^{water} \times \phi^{water} + \delta_d^{ethanol} \times \phi^{ethanol}$$

$$= 15.5 \times 0.44 + 15.8 \times 0.56$$

$$= 15.668$$

$$\delta_p = \delta_p^{water} \times \phi^{water} + \delta_p^{ethanol} \times \phi^{ethanol}$$

$$= 16 \times 0.44 + 8.8 \times 0.56$$

$$= 11.968$$

$$\delta_h = \delta_h^{water} \times \phi^{water} + \delta_h^{ethanol} \times \phi^{ethanol}$$

$$= 42.3 \times 0.44 + 19.4 \times 0.56$$

$$= 29.476$$

Hence, overall solubility parameter of solvent mixture, δ_{mix} , can be calculated as follows:

$$\begin{aligned}
\delta_{mix} &= (\delta_d^2 + \delta_p^2 + \delta_h^2)^{1/2} \\
&= (15.668^2 + 11.968^2 + 29.476^2)^{1/2} \\
&= 35.46 \text{ (MPa)}^{1/2}
\end{aligned}$$

B.3 Solubility Parameter Difference Calculation ($\Delta\delta$)

NMP is used as example to determine solubility parameter difference of solvent and coagulant mixtures consist of water/ethanol, and solubility parameter difference between solvent and polymer, PSf.

Solubility parameter of solvent (NMP)

$$\delta_d = 18 ; \delta_p = 12.3 ; \delta_h = 7.2 ; \delta_{mix} = 22.96$$

Solubility parameter of coagulant :

$$\delta_d = 15.668 ; \delta_p = 11.968 ; \delta_h = 29.476 ; \delta = 35.46$$

Solubility parameter of PSf:

$$\delta_d = 21.5 ; \delta_p = 2.8 ; \delta_h = 6.8 ; \delta = 22.72$$

Solubility parameter difference between NMP and coagulant, can be calculated as follows:

$$\begin{aligned}
\Delta\delta &= \sqrt{(\delta_{d,NMP} - \delta_{d,coagulant})^2 + (\delta_{p,NMP} - \delta_{p,coagulant})^2 + (\delta_{h,NMP} - \delta_{h,coagulant})^2} \\
&= \sqrt{(18 - 15.668)^2 + (12.3 - 11.968)^2 + (7.2 - 29.476)^2} \\
&= 22.4
\end{aligned}$$

Solubility parameter difference between solvent (NMP) and PSf, can be calculated as follows:

$$\begin{aligned}
\Delta\delta &= \sqrt{(\delta_{d,NMP} - \delta_{d,PSf})^2 + (\delta_{p,NMP} - \delta_{p,PSf})^2 + (\delta_{h,NMP} - \delta_{h,PSf})^2} \\
&= \sqrt{(18 - 21.5)^2 + (12.30 - 2.8)^2 + (7.2 - 6.8)^2} \\
&= 10.13 \text{ (MPa)}^{1/2}
\end{aligned}$$

APPENDIX C: POROSITY CALCULATION

C.1 Thickness of Membrane

Thickness of membrane measured at ten different points using micrometer gauge. The measured thickness is presented in Table C.1. Membrane area used for thickness measurement is kept constant at 25 cm² (L = 5 cm and W = 5 cm) for every samples

Table C.1 Thickness of membrane measured using SEM

Membrane preparation parameter	Mass (g)	Thickness (μm)
NMP 100w%	0.1157	91.27
NMP 75 w% / DCM 25 w%	0.0900	69.78
NMP 50 w% / DCM 50 w%	0.0743	54.57
DCM 100 w%	0.070	40.05

C.2 Membrane Overall Porosity Calculation

NMP membrane was taken as an example for overall porosity calculation. Based on SEM, NMP membrane has a thickness, l , of around 91.27 μm. Mass of membrane, m , was 0.1157 g and effective area of membrane measured, A , was 25 cm². With PSf density of 1.24 g/cm³, overall porosity of membrane, ε , can be calculated as follows:

$$\begin{aligned}\varepsilon &= \frac{V_{void}}{V_{tot}} \\ &= \frac{V_{tot} - V_{pol}}{V_{tot}} \\ &= \frac{lA - (m / \rho)}{lA}\end{aligned}$$

$$= \frac{0.009127 \times 25 - (0.1157 / 1.24)}{0.009127 \times 25}$$

$$= 0.5911$$

$$\varepsilon(\%) = 0.5911 \times 100\%$$

$$= 59.11\%$$

APPENDIX D: COAGULATION VALUE

D.1. Coagulation Value at Various Solvent – Non-solvent Pair

Result of titration method to determine the coagulation value of solution at different solvent mixtures is tabulated at Table D.1

Table D.1 Coagulation value of different solvent mixtures

Solution	Coagulation value (ml)		
	Run 1	Run 2	Average
NMP 100w%	6.4	6.5	6.5
NMP 75 w% / DCM 25 w%	7.5	7.3	7.4
NMP 50 w% / DCM 50 w%	9.2	9.3	9.3
DCM 100 w%	12.4	12.0	12.2

APPENDIX E: GAS PERMEATION

E.1 Gas Permeance and CO₂/CH₄ Ideal Calculations

Permeance of gases was measured by considering the time taken to flow certain amount of gas volume in bubble soap flow meter. As an example, for NMP membrane, time taken to flow 15 ml of CO₂ was 17.1 seconds at 1 barg feed pressure. The effective area of membrane, A , is 14.5 cm² and testing temperature is 25°C. Hence the permeance of CO₂ gas can be determined as follows:

$$\begin{aligned}\text{CO}_2 \text{ volumetric flow rate, } Q, &= \frac{\Delta V}{\Delta t_{\text{CO}_2}} \\ &= \frac{15}{17.1} \\ &= 0.8772 \text{ cm}^3/\text{s}\end{aligned}$$

This volumetric flow rate, Q , is corrected to standard temperature and pressure (STP), Q_{STP} , as follows:

$$\begin{aligned}\frac{V_{(\text{STP})}}{V_{300\text{K}}} &= \frac{273\text{K}}{398\text{K}} \\ Q &= \frac{V}{t} \\ \frac{Q_{(\text{STP})}}{Q_{300\text{K}}} &= \frac{273\text{K}}{398\text{K}} \\ Q_{\text{STP}} &= \frac{273\text{K}}{398\text{K}} \times 0.8772 \\ &= 0.8036 \text{ cm}^3 (\text{STP}) / \text{s}\end{aligned}$$

CO₂ flux, J_{CO_2} , is, therefore,

$$\begin{aligned}J_{\text{CO}_2} &= \frac{Q_{\text{STP}}}{A} \\ &= \frac{0.8036}{14.5} \\ &= 0.05542 \text{ cm}^3 (\text{STP}) / \text{cm}^2 \cdot \text{s}\end{aligned}$$

Once CO₂ flux, J_{CO_2} , was determined, the CO₂ permeance, $\frac{P}{l}$, can be calculated using the following formula:

$$\begin{aligned}
 \frac{P}{l} &= \frac{J_{CO_2}}{\Delta p} \\
 &= \frac{0.05542 \frac{cm^3 (STP)}{cm^2.s}}{1bar \times 76 \frac{cmHg}{bar}} \\
 &= 729 \times 10^{-6} \frac{cm^3 (STP)}{cm^2.cmHg.s} \\
 &= 729 GPU
 \end{aligned}$$

Similarly, CH₄ permeance, $\frac{P}{l}$, can be calculated using the same method. For NMP membrane, CH₄ permeance obtained is 107 GPU. CO₂/CH₄ ideal selectivity, α_{CO_2/CH_4} , can be calculated by dividing CO₂ permeance over CH₄ permeance as follows:

$$\begin{aligned}
 \alpha_{CO_2/CH_4} &= \frac{P/l_{CO_2}}{P/l_{CH_4}} \\
 &= \frac{729}{107} \\
 &= 6.81
 \end{aligned}$$

Table E.1. Gas permeation results for NMP 100 w% membrane

Membrane number	Run number	P(bar)	t _{CO2} (s)	t _{CH4} (s)	A (cm ²)	V (cm ³)	Q _{CO2} (cm ³ (STP)/s)	Q _{CH4} (cm ³ (STP)/s)	(P/I)CO ₂ (GPU)	(P/I)CH ₄ (GPU)	Selectivity CO ₂ /CH ₄
M1	1	1	17.6	115.3	14.5	15	0.7807733	0.1191814	708.50575	108.15005	6.5511364
	2	1	17.5	117.3	14.5	15	0.7852349	0.1171493	712.55436	106.30606	6.7028571
M2	1	1	16.9	116.5	14.5	15	0.8131131	0.1179537	737.85214	107.03606	6.8934911
	2	1	16.5	116.9	14.5	15	0.8328249	0.1175501	755.73947	106.66981	7.0848485
Average			17.1	116.5	14.5	15.0	0.8	0.1	728.7	107.0	6.8
RSD (%)			3.0	0.7	0.0	0.0	3.1	0.7	3.1	0.7	3.4
M1	1	2	13.4	55.9	14.5	15	1.0254933	0.2458249	465.28736	111.53579	4.1716418
	2	2	13.8	56.1	14.5	15	0.9957689	0.2449485	451.80077	111.13816	4.062174
M2	1	2	12.6	55.4	14.5	15	1.090604	0.2480435	494.82941	112.54243	4.3968254
	2	2	12.4	55.9	14.5	15	1.1081944	0.2458249	502.81053	111.53579	4.5080645
Average			13.1	55.8	14.5	15.0	1.1	0.2	478.7	111.7	4.3
RSD (%)			5.1	0.5	0.0	0.0	5.0	0.5	5.0	0.5	4.7
M1	1	3	9.5	32.4	14.5	15	1.4464853	0.4241238	437.53338	128.28911	3.4105263
	2	3	9.8	32.2	14.5	15	1.4022052	0.4267581	424.1395	129.08593	3.2857143
M2	1	3	9.9	32.9	14.5	15	1.3880415	0.4176781	419.85526	126.33942	3.3232323
	2	3	8.9	33.1	14.5	15	1.5440012	0.4151544	467.03001	125.57604	3.7191011
Average			9.5	32.7	14.5	15.0	1.4	0.4	437.1	127.3	3.4
RSD (%)			4.7	1.3	0.0	0.0	4.9	1.3	4.9	1.3	5.7
M1	1	4	7.6	10.1	14.5	15	1.8081067	1.3605555	410.18754	308.65597	1.3289474
	2	4	7.7	9.9	14.5	15	1.7846248	1.3880415	404.86043	314.89144	1.2857143
M2	1	4	7.0	9.8	14.5	15	1.9630872	1.4022052	445.34647	318.10462	1.4
	2	4	7.4	9.7	14.5	15	1.8569744	1.4166609	421.27369	321.38405	1.3108108
Average			7.4	9.9	14.5	15.0	1.9	1.4	420.4	315.8	1.3
RSD (%)			4.2	1.7	0.0	0.0	4.3	1.7	4.3	1.7	3.7
M1	1	5	6.6	7.4	14.5	15	2.0820622	1.8569744	377.86973	337.01895	1.1212121
	2	5	6.1	7.5	14.5	15	2.2527231	1.8322148	408.84266	332.52537	1.2295082
M2	1	5	6.4	7.2	14.5	15	2.1471267	1.908557	389.67816	346.38059	1.125
	2	5	5.9	7.3	14.5	15	2.3290866	1.8824124	422.70174	341.63565	1.2372881
Average			6.3	7.4	14.5	15.0	2.2	1.9	399.8	339.4	1.2
RSD (%)			5.0	1.8	0.0	0.0	5.0	1.8	5.0	1.8	5.4

Membrane number	Run number	P(bar)	t _{CO2} (s)	t _{CH4} (s)	A (cm ²)	V (cm ³)	Q _{CO2} (cm ³ (STP)/s)	Q _{CH4} (cm ³ (STP)/s)	(P/I)CO ₂ (GPU)	(P/I)CH ₄ (GPU)	Selectivity CO ₂ /CH ₄
M1	1	1	25.3	122.6	14.5	15	0.5431467	0.1120849	492.87357	101.71045	4.8458498
	2	1	25.7	123.7	14.5	15	0.534693	0.1110882	485.20238	100.80599	4.8132296
M2	1	1	24.9	121.5	14.5	15	0.5518719	0.1130997	500.79121	102.63129	4.8795181
	2	1	24.7	121.9	14.5	15	0.5563405	0.1127286	504.8462	102.29451	4.9352227
Average			25.2	122.4	14.5	15.0	0.5	0.1	495.9	101.9	4.9
RSD (%)			1.8	0.8	0.0	0.0	1.8	0.8	1.8	0.8	1.1
M1	1	2	15.4	61.5	14.5	15	0.8923124	0.2234408	404.86043	101.37968	3.9935065
	2	2	15.9	60.0	14.5	15	0.8642522	0.2290268	392.12897	103.91418	3.7735849
M2	1	2	15.2	60.3	14.5	15	0.9040533	0.2278874	410.18754	103.39719	3.9671053
	2	2	15.5	61.6	14.5	15	0.8865555	0.2230781	402.24843	101.21511	3.9741935
Average			15.5	60.9	14.5	15.0	0.9	0.2	402.4	102.5	3.9
RSD (%)			1.9	1.3	0.0	0.0	1.9	1.3	1.9	1.3	2.6
M1	1	3	12.9	34.4	14.5	15	1.0652411	0.3994654	322.2145	120.83044	2.6666667
	2	3	12.4	34.8	14.5	15	1.1081944	0.3948739	335.20702	119.44158	2.8064516
M2	1	3	12.1	34.7	14.5	15	1.1356703	0.3960118	343.51794	119.78579	2.8677686
	2	3	11.7	34.5	14.5	15	1.1744966	0.3983076	355.26214	120.4802	2.9487179
Average			12.3	34.6	14.5	15.0	1.1	0.4	339.1	120.1	2.8
RSD (%)			4.1	0.5	0.0	0.0	4.1	0.5	4.1	0.5	4.2
M1	1	4	9.8	12.0	14.5	15	1.4022052	1.1451342	318.10462	259.78544	1.2244898
	2	4	9.4	12.1	14.5	15	1.4618735	1.1356703	331.64099	257.63845	1.287234
M2	1	4	9.1	12.2	14.5	15	1.5100671	1.1263615	342.57421	255.52666	1.3406593
	2	4	9.8	11.9	14.5	15	1.4022052	1.1547572	318.10462	261.96851	1.2142857
Average			9.5	12.1	14.5	15.0	1.4	1.1	327.6	258.7	1.3
RSD (%)			3.6	1.1	0.0	0.0	3.6	1.1	3.6	1.1	4.7
M1	1	5	9.0	8.7	14.5	15	1.5268456	1.5794955	277.10447	286.6598	0.9666667
	2	5	9.2	8.4	14.5	15	1.4936533	1.635906	271.08046	296.89765	0.9130435
M2	1	5	9.5	8.8	14.5	15	1.4464853	1.5615467	262.52003	283.4023	0.9263158
	2	5	9.4	9.0	14.5	15	1.4618735	1.5268456	265.31279	277.10447	0.9574468
Average			9.3	8.7	14.5	15.0	1.5	1.6	269.0	286.0	0.9
RSD (%)			2.4	2.9	0.0	0.0	2.4	2.9	2.4	2.9	2.7

Membrane number	Run number	P(bar)	t _{CO2} (s)	t _{CH4} (s)	A (cm ²)	V (cm ³)	Q _{CO2} (cm ³ (STP)/s)	Q _{CH4} (cm ³ (STP)/s)	(P/I)CO ₂ (GPU)	(P/I)CH ₄ (GPU)	Selectivity CO ₂ /CH ₄
M1	1	1	20.0	73.2	14.5	0.5	0.0229027	0.0062576	20.782835	5.6783703	3.66
	2	1	19.9	72.4	14.5	0.5	0.0230178	0.0063267	20.887272	5.7411147	3.638191
M2	1	1	21.3	73.1	14.5	0.5	0.0215049	0.0062661	19.514399	5.6861383	3.4319249
	2	1	22.4	73.9	14.5	0.5	0.0204488	0.0061983	18.556103	5.6245833	3.2991071
Average			20.9	73.2	14.5	0.5	0.0	0.0	19.9	5.7	3.5
RSD (%)			5.7	0.8	0.0	0.0	5.6	0.8	5.6	0.8	4.9
M1	1	2	15.4	33.2	14.5	0.5	0.0297437	0.0137968	13.495348	6.2598902	2.1558442
	2	2	15.2	35.7	14.5	0.5	0.0301351	0.0128306	13.672918	5.8215225	2.3486842
M2	1	2	15.1	35.6	14.5	0.5	0.0303347	0.0128667	13.763467	5.8378751	2.3576159
	2	2	15.7	34.9	14.5	0.5	0.0291754	0.0131247	13.237475	5.9549672	2.2292999
Average			15.4	34.9	14.5	0.5	0.0	0.0	13.5	6.0	2.3
RSD (%)			1.7	3.3	0.0	0.0	1.7	3.4	1.7	3.4	4.3
M1	1	3	11.2	20.6	14.5	0.5	0.0408977	0.0222356	12.370735	6.7258367	1.8392857
	2	3	11.1	21.4	14.5	0.5	0.0412661	0.0214044	12.482183	6.4744035	1.9279279
M2	1	3	11.7	20.9	14.5	0.5	0.0391499	0.0219164	11.842071	6.6292936	1.7863248
	2	3	11.5	21.6	14.5	0.5	0.0398308	0.0212062	12.04802	6.4144554	1.8782609
Average			11.4	21.1	14.5	0.5	0.0	0.0	12.2	6.6	1.9
RSD (%)			2.4	2.2	0.0	0.0	2.4	2.2	2.4	2.2	3.2
M1	1	4	11.1	13.9	14.5	0.5	0.0412661	0.0329535	9.3616375	7.4758401	1.2522523
	2	4	10.8	13.2	14.5	0.5	0.0424124	0.034701	9.621683	7.8722861	1.2222222
M2	1	4	10.7	13.1	14.5	0.5	0.0428088	0.0349659	9.7116053	7.9323799	1.2242991
	2	4	10.5	12.7	14.5	0.5	0.0436242	0.0360672	9.8965883	8.1822186	1.2095238
Average			10.8	13.2	14.5	0.5	0.0	0.0	9.6	7.9	1.2
RSD (%)			2.3	3.8	0.0	0.0	2.3	3.7	2.3	3.7	1.5
M1	1	5	9.8	8.0	14.5	0.5	0.0467402	0.0572567	8.4827899	10.391418	0.8163265
	2	5	9.9	8.1	14.5	0.5	0.046268	0.0565498	8.3971052	10.263129	0.8181818
M2	1	5	10.1	7.9	14.5	0.5	0.0453519	0.0579815	8.2308259	10.522955	0.7821782
	2	5	9.6	8.3	14.5	0.5	0.0477139	0.0551872	8.6595147	10.015824	0.8645833
Average			9.9	8.1	14.5	0.5	0.0	0.1	8.4	10.3	0.8
RSD (%)			2.1	2.1	0.0	0.0	2.1	2.1	2.1	2.1	4.1

Membrane number	Run number	P(bar)	t _{CO2} (s)	t _{CH4} (s)	A (cm ²)	V (cm ³)	Q _{CO2} (cm ³ (STP)/s)	Q _{CH4} (cm ³ (STP)/s)	(P/I)CO ₂ (GPU)	(P/I)CH ₄ (GPU)	Selectivity CO ₂ /CH ₄
M1	1	1	44.1	104.6	14.5	0.5	0.0103867	0.0043791	9.4253222	3.9737735	2.3718821
	2	1	44.2	105.3	14.5	0.5	0.0103632	0.00435	9.4039979	3.9473571	2.3823529
M2	1	1	42.1	104.9	14.5	0.5	0.0108801	0.0043666	9.8730809	3.962409	2.4916865
	2	1	44.9	105.5	14.5	0.5	0.0102016	0.0043417	9.2573877	3.939874	2.3496659
Average			43.8	105.1	14.5	0.5	0.0	0.0	9.5	4.0	2.4
RSD (%)			2.7	0.4	0.0	0.0	2.8	0.4	2.8	0.4	2.6
M1	1	2	25.4	50.3	14.5	0.5	0.0180336	0.0091064	8.1822186	4.1317764	1.980315
	2	2	25.5	53.1	14.5	0.5	0.0179629	0.0086262	8.1501315	3.913905	2.0823529
M2	1	2	26.4	51.3	14.5	0.5	0.0173505	0.0089289	7.8722861	4.051235	1.9431818
	2	2	25.0	52.4	14.5	0.5	0.0183221	0.0087415	8.3131341	3.96619	2.096
Average			25.6	51.8	14.5	0.5	0.0	0.0	8.1	4.0	2.0
RSD (%)			2.3	2.4	0.0	0.0	2.3	2.4	2.3	2.4	3.7
M1	1	3	17.4	32.4	14.5	0.5	0.0263249	0.0141375	7.9627722	4.2763036	1.862069
	2	3	17.6	31.7	14.5	0.5	0.0260258	0.0144496	7.8722861	4.370733	1.8011364
M2	1	3	16.7	32.9	14.5	0.5	0.0274284	0.0139226	8.2965411	4.2113142	1.9700599
	2	3	17.7	32.4	14.5	0.5	0.0258787	0.0141375	7.8278099	4.2763036	1.8305085
Average			17.4	32.4	14.5	0.5	0.0	0.0	8.0	4.3	1.9
RSD (%)			2.6	1.5	0.0	0.0	2.7	1.5	2.7	1.5	4.0
M1	1	4	15.8	18.3	14.5	0.5	0.0289907	0.0250303	6.5768466	5.6783703	1.1582278
	2	4	15.9	18.8	14.5	0.5	0.0288084	0.0243646	6.5354828	5.5273498	1.1823899
M2	1	4	15.4	19.5	14.5	0.5	0.0297437	0.0234899	6.7476738	5.3289321	1.2662338
	2	4	15.8	18.1	14.5	0.5	0.0289907	0.0253068	6.5768466	5.7411147	1.1455696
Average			15.7	18.7	14.5	0.5	0.0	0.0	6.6	5.6	1.2
RSD (%)			1.4	3.3	0.0	0.0	1.4	3.3	1.4	3.3	4.6
M1	1	5	14.3	12.3	14.5	0.5	0.0320317	0.0372401	5.8133805	6.7586456	0.8601399
	2	5	14.4	12.4	14.5	0.5	0.0318093	0.0369398	5.7730098	6.7041404	0.8611111
M2	1	5	14.4	12.9	14.5	0.5	0.0318093	0.035508	5.7730098	6.44429	0.8958333
	2	5	14.2	12.2	14.5	0.5	0.0322573	0.0375454	5.8543198	6.8140444	0.8591549
Average			14.3	12.5	14.5	0.5	0.0	0.0	5.8	6.7	0.9
RSD (%)			0.7	2.5	0.0	0.0	0.7	2.4	0.7	2.4	2.1

APPENDIX F: MECHANICAL STRENGTH –UTM RESULTS

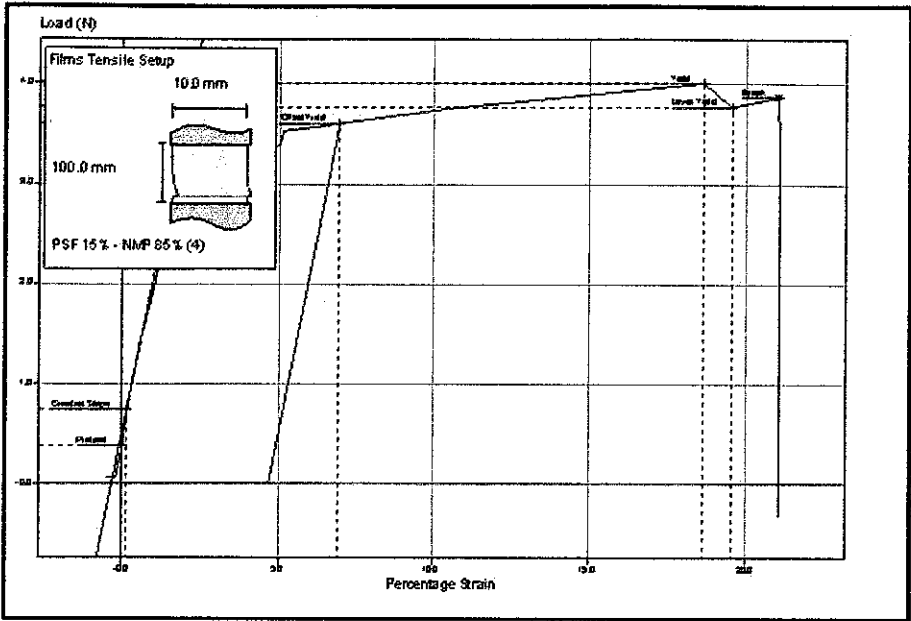


Figure F.1 (a) Tensile Test for NMP 100w%

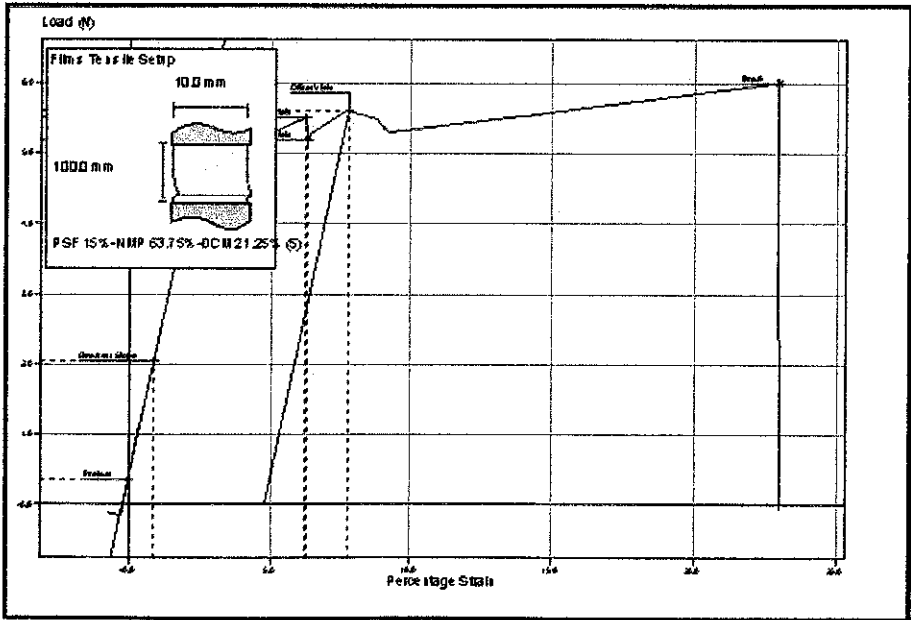


Figure F.1 (b) Tensile Test for NMP 75w%/DCM 25w%

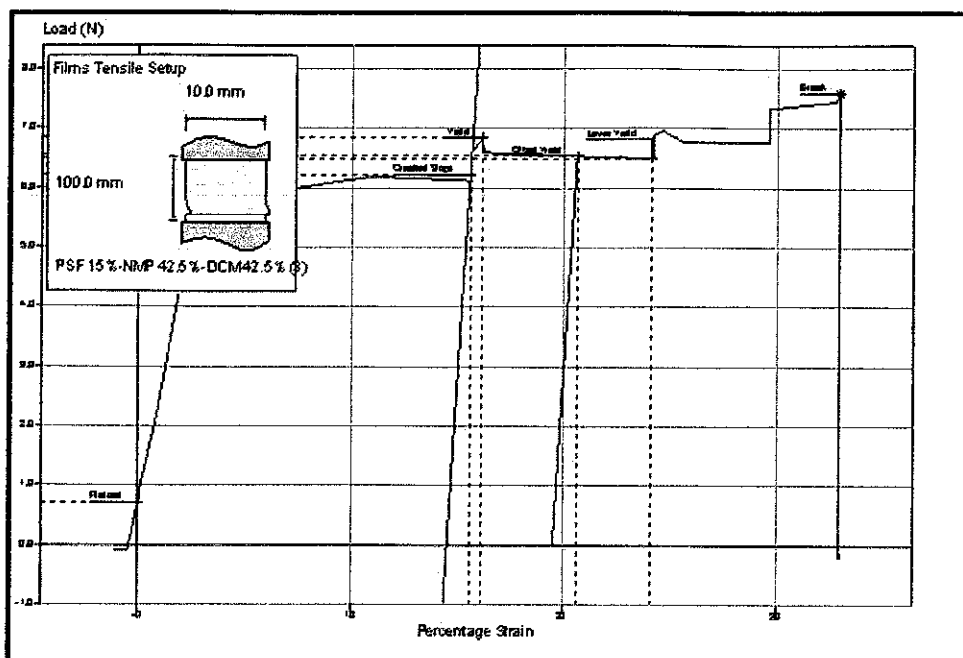


Figure F.1 (c) Tensile Test for NMP 50w%/DCM 50w%

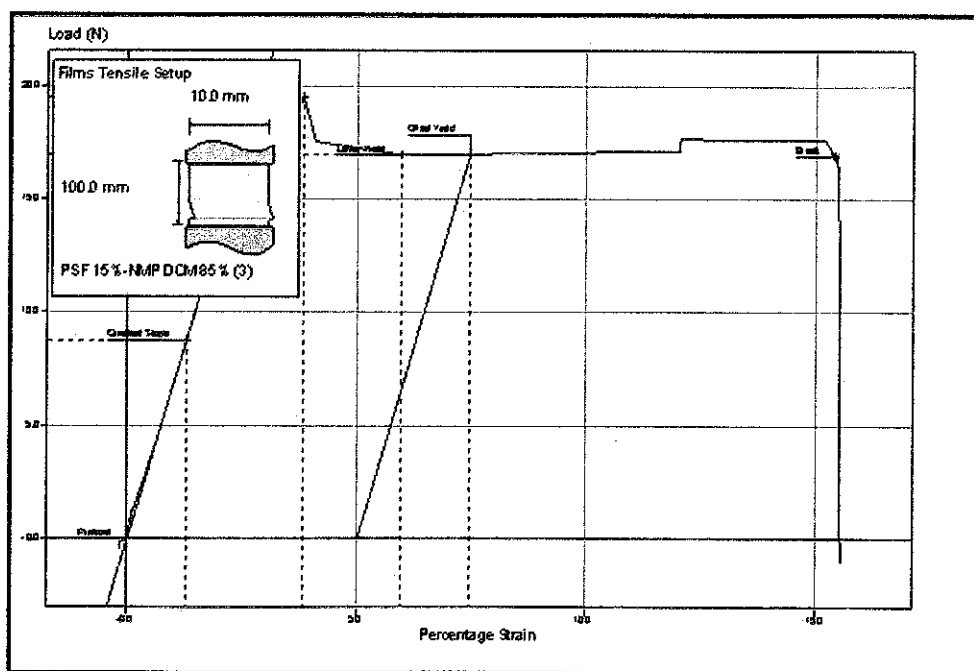
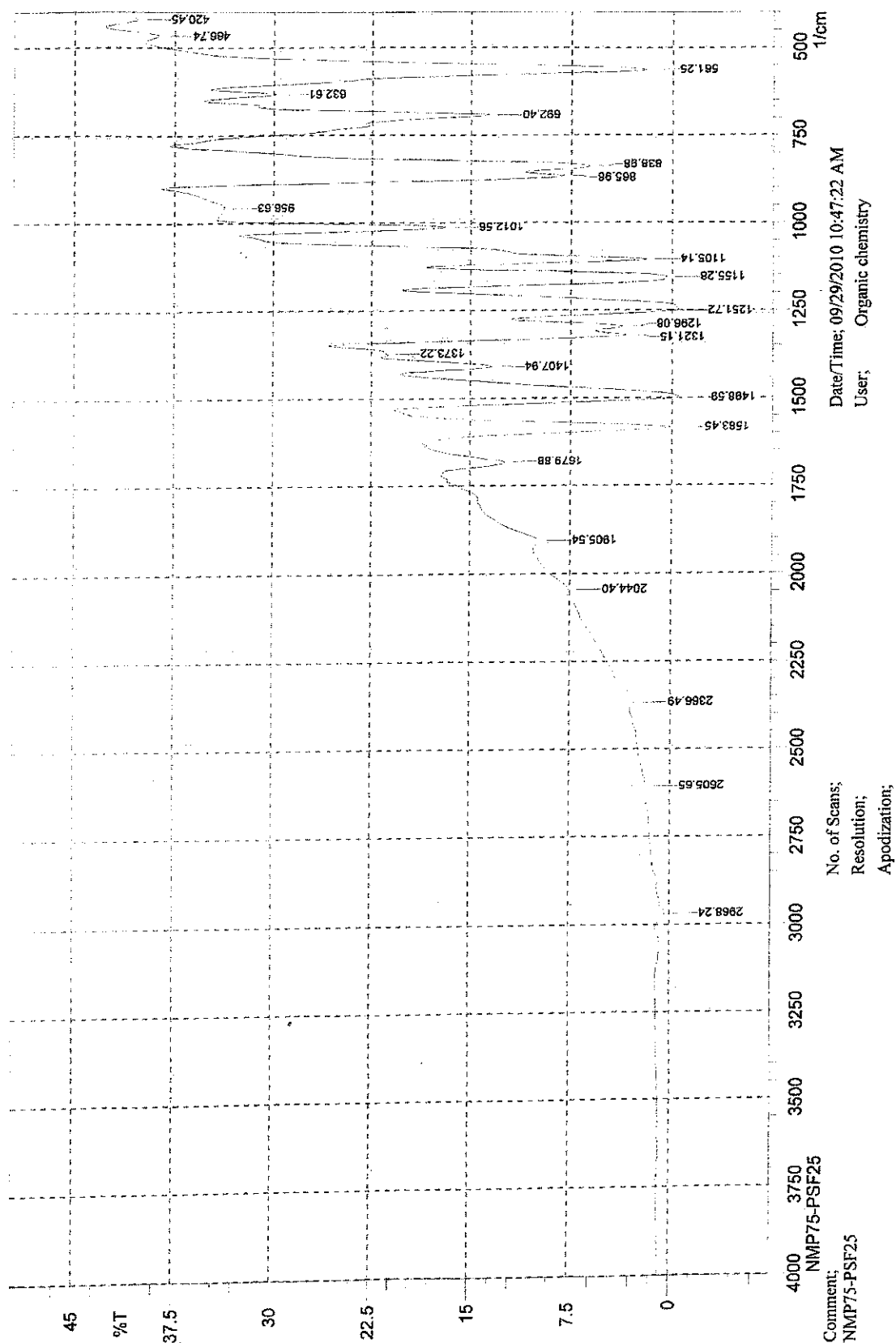
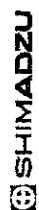
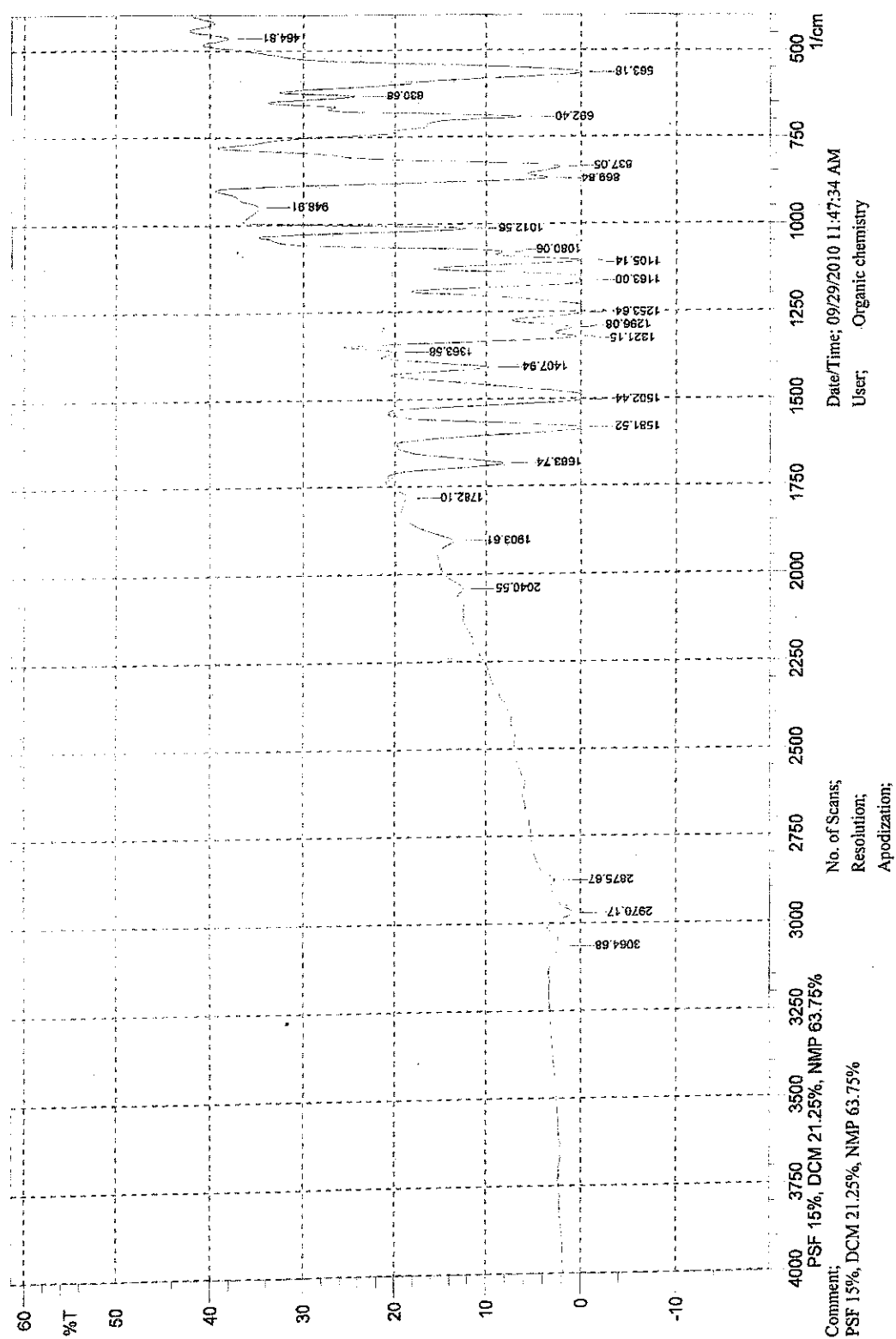


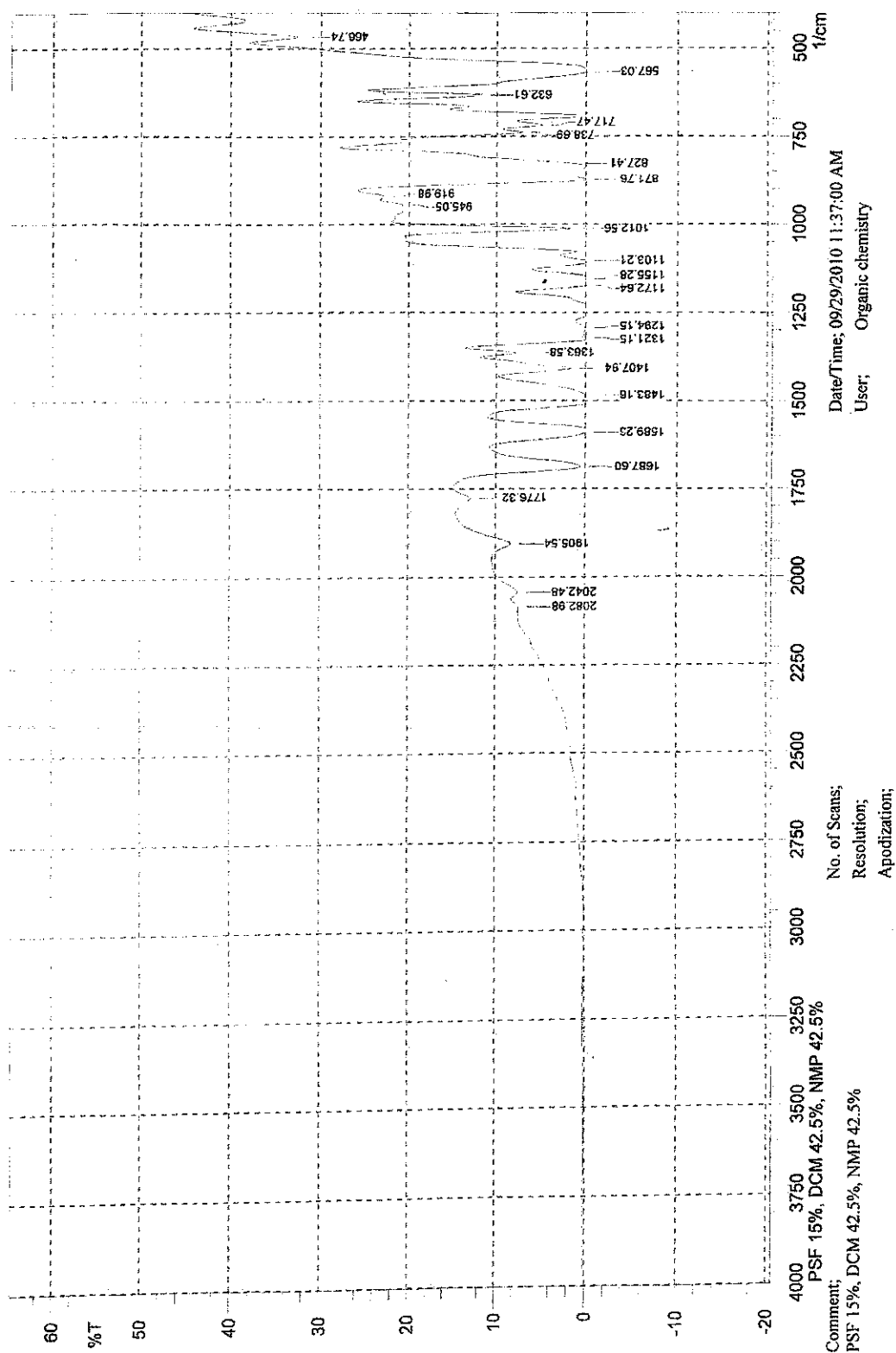
Figure F.1(d) Tensile Test for DCM 100w%.

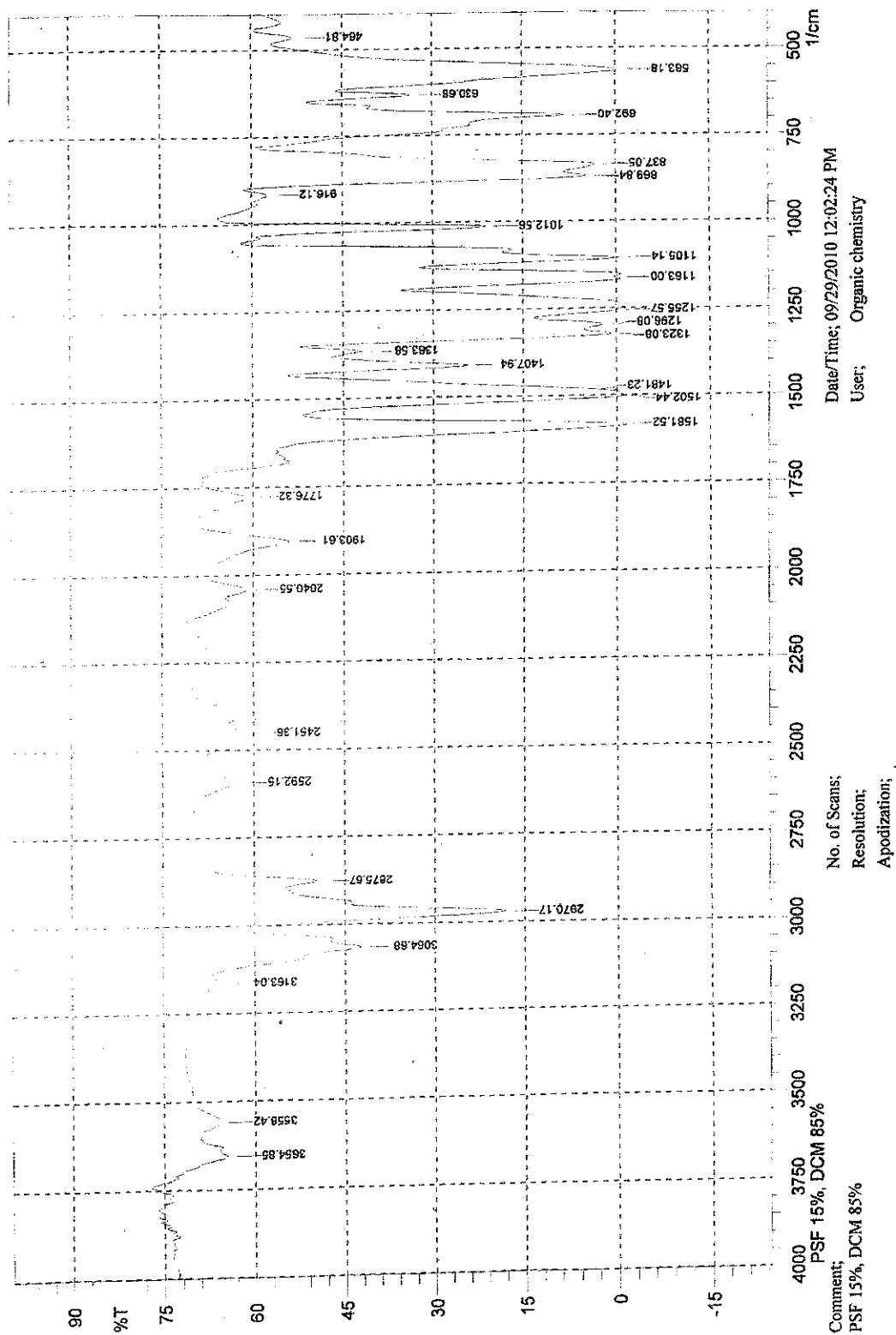
Sample Reference	Width (mm)	Sample Passed	Percentage Strain at Lower Yield	Load at Lower Yield (N)	Extension at Lower Yield (mm)	Initial Grip Separation (mm)
NMP 100w%	10	TRUE	19.5227969	3.771019575	19.61505538	100
NMP 75w%/DCM 25w%	10	TRUE	6.293536582	5.194487793	6.339206813	100
NMP 50w%/DCM 50w%	10	TRUE	24.15606865	6.487249063	24.42752817	100
DCM 100 w%	10	TRUE	5.969916201	16.9297052	5.978770282	100
Sample Reference	Speed (mm/min)	Preload Force (N)	Corrected Gauge Length (mm)	Load at Offset Yield (N)	Extension at Maximum Load (mm)	Extension at Break (mm)
NMP 100w%	50	1	100.472568	3.604012983	18.71445713	21.11429339
NMP 75w%/DCM 25w%	50	1	100.7256688	5.603289907	23.10586504	23.10586504
NMP 50w%/DCM 50w%	50	1	101.1237736	6.536047353	33.24391744	33.24391744
DCM 100 w%	50	1	100.1483116	16.97857821	3.829037058	15.40741671
Sample Reference	Break	Stiffness (N/m)	Percentage Strain at Offset Yield	Extension at Yield (mm)	Percentage Strain at Maximum Load	Strength at Maximum Load (N/m)
NMP 100w%	TRUE	1575.073043	6.958265631	18.71445713	18.62643457	400.7615306
NMP 75w%/DCM 25w%	TRUE	1862.828031	7.765359824	6.272544631	22.93940097	600.988913
NMP 50w%/DCM 50w%	TRUE	5860.420851	20.64048567	16.36064252	32.87448268	760.2075637
DCM 100 w%	TRUE	6884.655226	7.485531001	3.829037058	3.82336656	1950.061044
Sample Reference	Maximum Load (N)	Load at Break (N)	Strength at Lower Yield (N/m)	Strength at Yield (N/m)	Extension at Offset Yield (mm)	Percentage Strain at Yield
NMP 100w%	4.007615306	3.871118668	377.1019575	400.7615306	6.991148165	18.62643457
NMP 75w%/DCM 25w%	6.00988913	6.00988913	519.4487793	551.062666	7.821710618	6.227354661
NMP 50w%/DCM 50w%	7.602075637	7.602075637	648.7249063	684.2757655	20.872438	16.17882911
DCM 100 w%	19.50061044	16.90499515	1692.97052	1950.061044	7.496632915	3.82336656
Sample Reference	Load at Yield (N)	Elastic Modulus (N/m)	Percentage Strain at Break	Strength at Break (N/m)	Strength at Offset Yield (N/m)	
NMP 100w%	4.007615306	15825.16334	21.01498331	387.1118668	360.4012983	
NMP 75w%/DCM 25w%	5.51062666	18763.45993	22.93940097	600.988913	560.3289907	
NMP 50w%/DCM 50w%	6.842757655	59262.78715	32.87448268	760.2075637	653.6047353	
DCM 100 w%	19.50061044	68948.6597	15.38459956	1690.499515	1697.857821	

APPENDIX G: FTIR RESULTS









REFERENCES

- Albrecht, W., Weigel, Th., Schossig- Tiedemann, M., Kneifel, K., Peinemann, K.V. and Paul, D. 2001, "Formation of hollow fiber membranes from poly(ether imide) at wet phase inversion using binary mixtures of solvents for the preparation of the dope," *J. Membr. Sci.* **192**: 217–230
- Baker, R. W. 1994, *Membrane technology and applications*, John Wiley & Son, Ltd
- Barton, A.F.M. 1985, *Handbook of solubility parameters and other cohesion parameters*, Florida, CRC press
- Bord, N., Cre´tier, G., Rocca, J. L., Bailly, C., and Souchez, J.P. 2004, "Determination of diethanolamine or N-methyldiethanolamine in high ammonium concentration matrices by capillary electrophoresis with indirect UV detection: application to the analysis of refinery process waters," *Anal Bioanal Chem* **380**: 325–332
- Chun, K.Y., Jang, S.H., Kim, H.S., Kim, Y.W., Han, H.K., and Joe, Y.I. 2000, "Effects of solvent on the pore formation in asymmetric 6FDA-4,4'ODA polyimide membrane: terms of thermodynamic, precipitation kinetics, and physical factors," *J. Membr. Sci.* **169** 197-214
- Dijk, M.A.V., and Wakker, A. 1997, *Concepts of polymer thermodynamics*, Lancaster, Basel, Technomic Publishing Co., Inc.
- Dortmundt, D., and Doshi, K. 1999, *Recent Developments in CO₂ Removal Membrane Technology*, USA, UOP LLC
- Ebewele, R.O. 2000, *Polymer Science and Technology*, Boca Raton, Florida, CRC press
- Gosh, M.K., and Mital, K.L. 1996, *Polyimides: Fundamental and Applications*, New York, Marcel Dekker, Inc

Han, M.J. 1999, *Desalination* (121): 31–39, 230, Korea

Hansen, C.M. 2000, *Hansen solubility parameter, A user's handbook.*, London, CRC press

Hwang, J.R., Koo, S.H., Kim, J.H., Higuchi and Tak, T.M. 1996, *Effects of casting solution composition on performance of PES membrane*, Korea; Japan

Iqbal, M. 2007, *Development of Asymmetric Polysulfone (PSF) Membrane for Carbon Dioxide Removal from Methane*, Master Degree Thesis, University Technology PETRONAS, Malaysia

Iqbal, M., Man, Z., Mukhtar, H. and Dutta, B.K. 2008, "Solvent effect on morphology and CO₂/CH₄ separation performance of asymmetric polysulfone membranes," *J. Membr. Sci.* **318** (1-2): 167–175

Ismail, A.F. and David, L.I.B. 2001, "A Review on the latest development of carbon membranes for gas separation," *J. Membr. Sci.* **193**: 1-18

Ismail, A.F. and Lorna, W. 2002, *Penetrant-induced plasticization phenomenon in glassy polymers for gas separation membrane*, Review article, *Sep. Purif. Tech.* **27**: 173–194

Ismail, A.F. and Lai, P.Y. 2004, *Development of Defect-Free Asymmetric Polysulfone Membranes for Gas Separation Using Response Surface Methodology*, *Sep. Purif. Technol.* **40**: 191.

Jansen, J.C., Macchione, M., and Drioli, E. 2005a, "High flux asymmetric gas separation membranes of modified poly(ether ether ketone) prepared by the dry phase inversion technique" *J. Membr. Sci.* **255**: 167-180

Jansen, J.C., Macchione, M., Oliviero, C., Mendichi, R., Ranieri, G.A., and Drioli, E. 2005b, "Rheological evaluation of the influence of polymer concentration and molar mass distribution on the formation and performance of asymmetric gas separation membranes prepared by dry phase inversion," *Polymer* **46**: 11366-11379

- Jordan, S.M., and Koros, W.J. 1990, "Characterization of CO₂-induced conditioning of substituted polycarbonates using various exchange penetrants," *J. Membr. Sci.* **51**: 233-247
- Kang, Y.S., Kim, H.J., Kim, Y.H. and Jo, W.H. 1988, *The mechanism of a asymmetric membrane formation via phase inversion process*, Seoul National University, Department of Textile Engineering
- Kesting, R. E. 1985, *Synthetic Polymeric Membrane 2*, New York, John Wiley & Sons
- Kesting, R.E. 1990, "The four tiers of structure in integrally skinned phase inversions membranes and their relevance to the various separation regimes," *J.Appl.Polym.Sci.*, **41**: 2739-2752
- Koenig, J.L. 1992, *Spectroscopy of Polymers, ACS Professional Reference Book*, Washington DC, American Chemical Society
- Kohl, A. and Riesenfeld, F. 1979, *Gas purification*, Houston, Texas, Gulf Publishing Company
- Koros, W.J., Chan, A.H., and Paul, D.R. 1977, "Sorption and transport of various gases in polycarbonate," *J. Membr. Sci.* **2**: 165-190
- Koros, W.J., Coleman, M.R, and Walker, D.R.B. 1992, "Controlled Permeability Polymer Membranes," *Ann. Rev. Sci.*, **22**: 47
- Koros, W.J., MA, Y.H. and Shimidzu, T. 1996, "Terminology for membranes and membrane processes," *Pure and Appl. Chem.*, **68**: 1479-1489
- Koros, W.J. and Mahajan, R. 2000, "Pushing the Limits on Possibilities for Large Scale Gas Separation: Which Strategies?," *J. Membr. Sci.* **175**: 181-196

Kravellen, D.W.V. 1990, *Properties of polymers: Their correlation with chemical structure; Their numerical estimation and prediction from additive group contribution (3)*, Amsterdam, Elsevier

Lakshminarayanaiah, N. 1985, *Equations of membrane biophysics*, New York, Academic Press

Li, J., Wang, S., Nagai, K., Nakagawa, T., and Mau, A.W.H. 1998, "Effect of polyethyleneglycol (PEG) on gas permeabilities and permselectivities in its cellulose acetate (CA) blend membranes," *J. Membr. Sci.* **138**: 143-152

Machado, P.S.T., Habert, A.C. and Borges, C.P. 1999, "Membrane formation mechanism based on precipitation kinetics and membrane morphology: flat and hollow fiber polysulfone membranes", *J. Membr. Sci.* **155**:171–183

Matsuyama, H., Yamamoto, A., Yano, H., Maki, T., Teramoto M., Mishima, K. and Matsuyama, K. 2002, "Effect of organic solvents on membrane formation by phase separation with supercritical CO₂," *J. Membr. Sci.* **204**: 81.

Mulder, M. 1996. *Basic Principles of Membrane Technology* (2), Kluwer Academic.

Mulder, M. 1997, *Basic Principles of Membrane Technology*, Netherlands. Kluwer Academic Publisher

Niwa, M., Kawakami, H., Nagaoka, S., Kanamori, T., and Shinbo, T. 2000, "Fabrication of an asymmetric polyimide hollow fiber with a defect-free surface skin layer," *J. Membr. Sci.* **171**: 253-261

Nunes, S.P., and Peinemann, K.V. 2001, *Membrane technology in the chemical industry*, Germany, WILEY-VCH

Peinemann, K.V., and Pinnau, I., *Method for producing an integral asymmetric gas separating membrane and the resultant membrane*, United States Patent Number 4,746,333, 1988

Reverchon, E., Schiavo Rappo, E. and Cardea, S. 2006, "Flexible supercritical CO₂- assisted process for poly(methyl methacrylate) structure formation," *Polym. Eng. Sci.* **46**: 188

Rodriguez, F., Cohen, C., Ober., C.K., and Archer, L.A. 2003, *Principles of polymer system (5)*, New York, Taylor & Francis Group

Ruthven, D.M. 1997, *Encyclopedia of separation technology (2): A Kirk-Othmer encyclopedia*, John Wiley & Sons

Sanders, E.S. 1988, "Penetrant-induced plasticization and gas permeation in glassy polymers," *J.Membr.Sci* **37**: 63-80

Shieh, J.J. and Chung, T.S. 1998, "Effect of liquid-liquid demixing on the membrane morphology, gas permeation, thermal and mechanical properties of cellulose acetate hollow fibers," *J. Membr. Sci.* **140**: 67-79

Strathmann. H., Kock, K. and Amar, P. 1975, "The formation mechanism of asymmetric membranes," *Desalination* **16**: 179-203

Strathmann. H., and Kock, K. 1977, "The formation mechanism of phase inversion membranes," *Desalination* **21**: 241-255

Strathmann, H. and Bauer, B. 1989, "7th European Summer School" in *Membrane Science*

Temtem, M., Casimiro, T. and Aguiar-Ricardo, A. 2006, *Solvent power and depressurization rate effects in the formation of polysulfone membranes with CO₂-assisted phase inversion method.*

Wang, Z.G., Xu, Z.K. and Wan, L.S., 2006, "Modulation the morphologies and performance of polyacrylonitrile-based asymmetric membranes containing reactive groups: Effect of non-solvents in the dope solution," *J. Membr. Sci.* **278**: 447-456

Wienk, M., OldeScholtenhuis, F.H.S., Boomgaard, T. and Smolders, C.A. 1995, *J. Membr. Sci.* **106**: 233–243

Yampolskii, Y., Pinnau, I. and Freeman, B.D. 2006, *Materials Science of Membranes for Gas and Vapor Separation*, John Wiley & Son, Ltd.

Yip, Y. and McHugh, A.J. 1006, “Modeling and simulation of nonsolvent vapor-induced phase separation,” *J. Membr. Sci* **271**: 163-176

Zydney, A.L. and Zeman, L.J. 1996, *Microfiltration and ultrafiltration: Principles and Applications*, New York.